Few-Class Arena: A BENCHMARK FOR EFFICIENT SELECTION OF VISION MODELS AND DATASET DIFFICULTY MEASUREMENT

Anonymous authors
Paper under double-blind review

ABSTRACT

We propose *Few-Class Arena* (*FCA*), as a unified benchmark with focus on testing efficient image classification models for few classes. A wide variety of benchmark datasets with many classes (80-1000) have been created to assist Computer Vision architectural evolution. An increasing number of vision models are evaluated with these many-class datasets. However, real-world applications often involve substantially fewer classes of interest (2-10). This gap between many and few classes makes it difficult to predict performance of the few-class applications using models trained on the available many-class datasets. To date, little has been offered to evaluate models in this *Few-Class Regime*. We conduct a systematic evaluation of the ResNet family trained on ImageNet subsets from 2 to 1000 classes, and test a wide spectrum of Convolutional Neural Networks and Transformer architectures over ten datasets by using our newly proposed *FCA* tool. Furthermore, to aid an up-front assessment of dataset difficulty and a more efficient selection of models, we incorporate a difficulty measure as a function of class similarity. *FCA* offers a new tool for efficient machine learning in the *Few-Class Regime*, with goals ranging from a new efficient class similarity proposal, to lightweight model architecture design, to a new scaling law. *FCA* is user-friendly and can be easily extended to new models and datasets, facilitating future research work. Our benchmark is available at https://github.com/fewclassarena/fca.

1 INTRODUCTION

The de-facto benchmarks for evaluating efficient vision models are large scale with many classes (e.g. 1000 in ImageNet (Deng et al., 2009), 80 in COCO (Lin et al., 2014), etc.). Such benchmarks have expedited the advance of vision neural networks toward efficiency (Tan & Le, 2019a; Tan & L., 2021; Sinha & El-Sharkawy, 2019; Sandler et al., 2018; Howard et al., 2019; Iandola et al., 2016; Ma et al., 2018; Mehta & Rastegari) with the hope of reducing the financial and environmental cost of vision models (Patterson et al., 2021; Rae et al., 2021). More efficient computation is facilitated by using quantization (Gysel et al., 2018; Han et al., 2015; Leng et al., 2018), pruning (Cheng et al., 2017; Blalock et al., 2020; Li et al., 2016; Shen et al., 2022), and data saliency (Yeung et al., 2016). Despite efficiency improvements such as these, many-class datasets are still the standard of model evaluation.

Real-world applications, however, typically comprise only a few number of classes (e.g, less than 10) (Shao et al., 2020; A. Delplanque, 2022; Cai et al., 2021) which we termed *Few-Class Regime*. This introduces a crucial research question: what is the simplest baseline model capable of meeting performance criteria within this *Few-Class Regime*? To deploy a vision model pre-trained on large datasets in a specific environment, it requires the re-evaluation of published models or even retraining to find an optimal model in an expensive architectural search space (Scheidegger et al., 2019).

One major finding is that, apart from scaling down model and architectural design for efficiency, dataset difficulty also plays a vital role in model selection (Scheidegger et al., 2021) (described in Section 4.3).
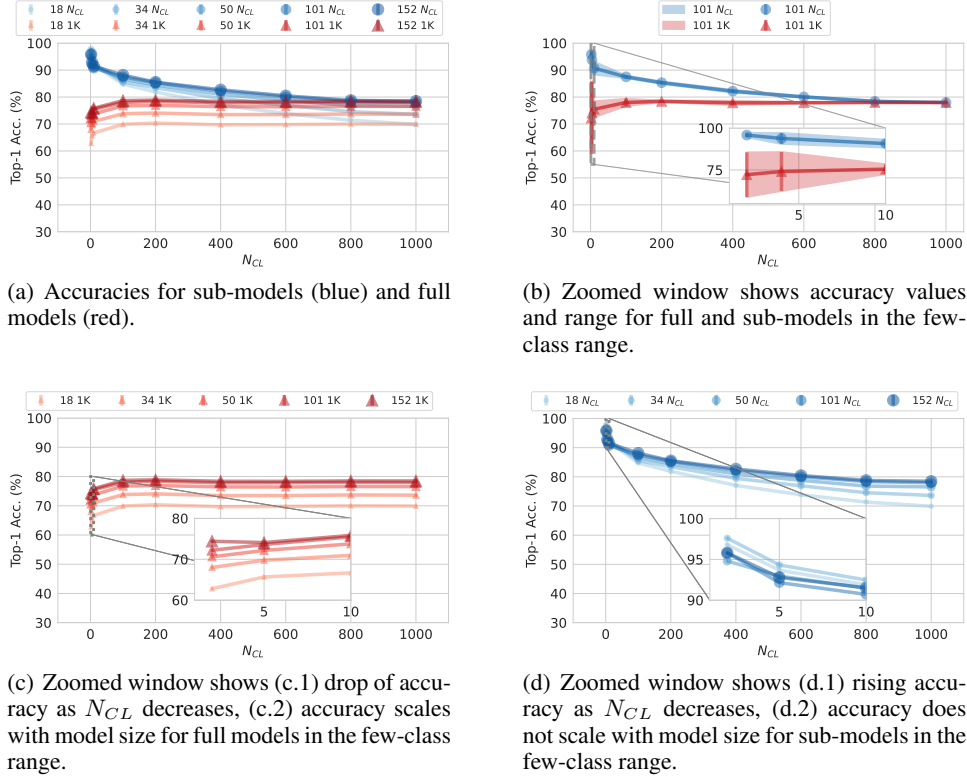
(a) Accuracies for sub-models (blue) and full models (red).

(b) Zoomed window shows accuracy values and range for full and sub-models in the few-class range.

(c) Zoomed window shows (c.1) drop of accuracy as N_{CL} decreases, (c.2) accuracy scales with model size for full models in the few-class range.

(d) Zoomed window shows (d.1) rising accuracy as N_{CL} decreases, (d.2) accuracy does not scale with model size for sub-models in the few-class range.

Figure 1: Top-1 accuracies of various scales of ResNet, whose model sizes are shown in the legend, and whose plots vary from dark to light by decreasing size. Plots range along number of classes N_{CL} from the full ImageNet size (1000) down to the *Few-Class Regime*. Each model is tested on 5 subsets whose N_{CL} classes are randomly sampled from the original 1000 classes. (a) Plots for sub-models trained on subsets of classes (blue) and full models trained on all 1000 classes (red). (b) Zoomed window shows the standard deviation of subset's accuracies is much smaller than for the full model. (c.1) Full model accuracies drop when N_{CL} decreases. (c.2) Full model accuracies increase as model scales up in the *Few-Class Regime*. (d.1) Sub-model accuracies grow as N_{CL} decreases. (d.2) Sub-model accuracies do not increase when model scales up in the *Few-Class Regime*.

Figure 1 summarizes several key findings under the *Few-Class Regime*. On the left graph in red are accuracy results for a range of number of classes N_{CL} for what we call the "full model", that is ResNet models pre-trained on the full 1000 classes of ImageNet (generally available from many websites). On the right are accuracy results for what we call "sub-models", each of which is trained and tested on the same N_{CL}, where this number of classes is sampled from the full dataset down to the *Few-Class Regime*. Findings include the following. (a) Sub-models attain higher upper-bound accuracy than full models. (b) The range of accuracy widens for full models at few-classes, which increases the uncertainty of a practitioner selecting a model for few classes. In contrast, sub-models narrow the range. (c) Full models follow the scaling law (Kaplan et al., 2020) in the dimension of model size - larger models (darker red) have higher accuracy from many to few classes. (d) Surprisingly, the scaling law is violated for sub-models in the *Few-Class Regime* (see the zoomed-in subplot) where larger models (darker blue) do not necessarily perform better than smaller ones (lighter blue). From these plots, our key insight is that, instead of using full models, researchers and practitioners in the *Few-Class Regime* should use sub-models for selection of more efficient models.

However, obtaining sub-models involves computationally expensive training and testing cycles since they need to be converged on each of the few-class subsets. By carefully studying and comparing the experiment and evaluation setup of these works in the literature, we observe that, how models scale down to *Few-Class Regime* is rarely studied. The lack of comprehensive benchmarks for *few-class* research impedes both researchers and practitioners from quickly finding models that are the most efficient for their dataset size. To fill this need, we propose a new benchmark, *Few-Class*

Arena (*FCA*), with the goal of benchmarking vision models under few-class scenarios. To our best knowledge, *FCA* is the first benchmark for such a purpose.

We formally define *Few-Class Regime* as a scenario where the dataset has a limited number of classes. Real-world applications often comprise only a few number of classes (e.g. $N_{CL} < 10$ or 10% classes of a dataset). Consequently, *Few-Class Arena* refers to a benchmark to conduct research experiments to compare models in the *Few-Class Regime*. This paper focuses on the image classification task, although *Few-Class Regime* can generalize to object detection (Chen et al., 2019) and other visual tasks.

Statement of Contributions. Four contributions are listed below:

- To the best of our knowledge, we are the first to explore the problems in the *Few-Class Regime* and develop a benchmark tool *Few-Class Arena* (*FCA*) to facilitate scientific research, analysis, and discovery for this range of classes.
- We introduce a scalable few-class data loading approach to automatically load images and labels in the *Few-Class Regime* from the full dataset, avoiding the need to duplicate data points for every additional few-class subset.
- We incorporate dataset similarity as an inverse difficulty measurement in *Few-Class Arena* and propose a novel Silhouette-based similarity score named *SimSS*. By leveraging the visual feature extraction power of CLIP and DINOv2, we show that *SimSS* is highly correlated with ResNet performance in the *Few-Class Regime* with high Pearson coefficient scores ≥ 0.88.
- We conduct extensive experiments that comprise ten models on ten datasets and 2-1000 numbers of classes on ImageNet, totalling 1591 training and testing runs. In-depth analyses on this large body of testing reveal new insights in the *Few-Class Regime*.

2 RELATED WORK

Visual Datasets and Benchmarks. To advance deep neural network research, a wealth of large-scale many-class datasets has been developed for benchmarking visual neural networks over a variety of tasks. Typical examples [1] include 1000 classes in ImageNet (Deng et al., 2009) for image classification, and 80 object categories in COCO (Lin et al., 2014) for object detection. Previous benchmarks also extend vision to multimodal research such as image-text (Lee et al., 2024; Le et al., 2024; Laurençon et al., 2024; Bitton et al., 2022). While prior works often scale up the number of object categories for general purpose comparison, studies (Fang et al., 2024; Mayo et al., 2023) raise a concern on whether models trained on datasets with such a large number of classes (e.g. ImageNet) can be reliably transferred to real world applications often with far fewer classes. A close work to ours is vision backbone comparison (Goldblum et al., 2024) whose focus is on model architectures. Our perspective differs in a focus on cases with fewer number of classes, which often better aligns with real-world scenarios.

Dataset Difficulty Measurement. Research has shown the existence of inherent dataset difficulty (Mayo et al., 2023) for classification and other analytic tasks. Efficient measurement methods are proposed to characterize dataset difficulty using Silhouette Score (Rousseeuw, 1987), K-means Fréchet inception distance (Dowson & Landau, 1982; Heusel et al., 2017; Lucic et al., 2018), and Probe nets (Scheidegger et al., 2021). Prior studies have proposed image quality metrics using statistical heuristics, including peak signal-to-noise ratio (PSNR) (Hore & Ziou, 2010), structural similarity (SSIM) Index (Wang et al., 2004), and visual information fidelity VIF (Sheikh & Bovik, 2006). A neuroscience-based image difficulty metric (Mayo et al., 2023) is defined as the minimum viewing time related to object solution time (OST) (Kar et al., 2019). Another type of difficulty measure method consists of additional procedures such as c-score (Jiang et al., 2020) , prediction depth (Baldock et al., 2021) , and adversarial robustness (Goodfellow et al., 2014) . Our work aligns with the line of research (Arun, 2012; Trick & Enns, 1998; Wolfe et al., 2010) involving similarity-based difficulty measurements: similar images are harder to distinguish from each other while dissimilar images are easier. Previous studies are mainly in the image retrieval context (Zhang & Lu, 2003; Wang et al., 2014; Tudor Ionescu et al., 2016). Similarity score is used in (Cao et al., 2023) with the limitation that a model serving similarity measurement has to be trained for one dataset. We

---

[1] A detailed list of many-class datasets used in this paper can be found in the Appendix.

push beyond this limit by leveraging large vision models that learn general visual features using CLIP (Radford et al., 2021) and DINOv2 (Oquab et al., 2023). The study (Mayo et al., 2023) shows that CLIP generalizes well to both easy and hard images, making it a good candidate for measuring image difficulty. Supported by the evidence that better classifiers can act as better perceptual feature extractors (Kumar et al., 2022), in later sections we show how CLIP and DINOv2 will be used as our similarity base function.

Despite the innovation of difficulty measure algorithms on many-class datasets, little attention has been paid to leveraging these methods in the *Few-Class Regime*. We show that, as the number of classes decreases, sub-dataset difficulty in the *Few-Class Regime* plays a more critical role in efficient model selection. To summarize, unlike previous work on many-class benchmarks and difficulty measurements, our work takes few-class and similarity-based dataset difficulty into consideration, and in doing so we believe the work pioneers the development of visual benchmark dedicated to research in the *Few-Class Regime*.

3   FEW-CLASS ARENA (FCA)

We introduce the *Few-Class Arena* (*FCA*) benchmark in this section. In practice, we have integrated *FCA* into the MMPreTrain framework (Contributors, 2023), implemented in Python3 and Pytorch[2]. Our benchmark usage guidelines are detailed in A.2 of the Appendix.

3.1   FEW-CLASS DATASET PREPARATION

Few-Class Arena provides an easy way to prepare datasets in the *Few-Class Regime*. By leveraging the MMPreTrain framework, users only need to specify the parameters of few-class subsets in the configuration files, which includes the list of models, datasets, number of classes (N_{CL}), and the number of seeds (N_S). *Few-Class Arena* generates the specific model and dataset configuration files for each subset, where subset classes are randomly extracted from the full set of classes, as specified by the seed number. Note that only one copy of the full, original dataset is maintained during the whole benchmarking life cycle because few-class subsets are created through the lightweight configurations, thus maximizing storage efficiency. We refer readers to the Appendix and the publicly released link for detailed implementations and use instructions.

3.2   MANY-CLASS FULL DATASET TRAINED BENCHMARK

We conducted large-scale experiments spanning ten popular vision models (including CNN and ViT architectures) and ten common datasets [3]. Except for ImageNet1K, where pre-trained model weights are available, we train models in other datasets from scratch. While different models' training procedures may incur various levels of complexity (particularly in our case for MobileNet V3 and Swin Transformer V2 base), we have endeavored to minimize changes in the existing training pipelines from MMPreTrain. The rationale is that if a model exhibits challenges in adapting it to a dataset, then it is often not a helpful choice for a practitioner to select for deployment.

Results are summarized in Table 1. We observe (1) models in different datasets (in rows) yield highly variable levels of performance by Top-1 accuracy; (2) no single best model (bold, in columns) exists across all datasets; and (3) model rankings vary across various datasets.

The first two observations are consistent with the findings in (Scheidegger et al., 2021; Fang et al., 2024). For (1), it suggests there exists underlying dataset-specific difficulty. To capture this characteristic, we adopt the reference dataset classification difficulty number (DCN) (Scheidegger et al., 2021) to refer to the empirically highest accuracy achieved in a dataset from a finite number of models shown in Table 1 and Figure 2 (a). For observation (3), we can examine the rankings among the

---

[2]Code is available at `https://github.com/fewclassarena/fca`, including detailed documentation and long-term plans of maintenance.

[3]Models include: ResNet50 (RN50), VGG16, ConvNeXt V2 (CNv2), Inception V3 (INCv3), EfficientNet V2 (EFv2), ShuffleNet V2 (SNv2), MobileNet V3 (MNv3), Vision Transformer base (ViTb), Swin Transformer V2 base (SWv2b) and MobileViT small (MViTs). Datasets include CalTech101 (CT101), CalTech256 (CT256), CIFAR100 (CF100), CUB200 (CB200), Food101 (FD101), GTSRB43, (GT43), ImageNet1K (IN1K), Indoor67 (ID67), Quickdraw345 (QD345) and Textures47 (TT47).

4

ten models of ResNet50 and EfficientNet V2 in Figure 2 (b). ResNet50's ranking varies dramatically for the different datasets, for instance ranking 7th on ImageNet1K and 1st on Quickdraw345. This ranking variability is also observed in other models (see all models in the Appendix). However, a common practice is to benchmark models – even for efficiency – on large datasets, especially ImageNet1K. The varied dataset rankings in our experiments expose the limitations of such a practice, further supporting our new benchmark paradigm, especially in the *Few-Class Regime*. In later sections, we leverage DCN and image similarity for further analysis.

Dataset	RN50	VGG16	CNv2	INCv3	EFv2	SNv2	MNv3	ViTb	SWv2b	MViTs	DCN
GT43	99.85	96.60	99.83	99.78	99.86	**99.87**	99.83	99.31	99.78	99.69	99.87
CF100	74.56	71.12	**85.89**	75.97	77.05	77.89	74.35	32.65	78.49	76.51	85.89
IN1K	76.55	71.62	84.87	77.57	**85.01**	69.55	66.68	82.37	84.6	78.25	85.01
FD101	83.76	75.82	63.80	83.96	80.82	79.36	76.03	52.21	**84.30**	82.23	84.30
CT101	77.70	74.99	77.52	77.52	77.82	**84.13**	80.71	59.59	78.82	80.06	84.13
CT256	65.07	59.08	**73.57**	66.09	62.80	68.13	62.62	44.23	67.28	65.80	73.57
QD345	**69.14**	19.86	62.86	68.25	68.81	67.32	66.42	19.67	66.54	68.76	69.14
CB200	45.86	21.26	27.61	45.58	44.48	53.95	53.80	23.73	54.52	**58.46**	58.46
ID67	53.75	26.01	33.21	45.95	43.85	**54.72**	51.65	30.51	48.58	54.05	54.72
TT47	30.43	12.55	6.49	14.20	21.17	**43.83**	40.27	31.38	33.94	24.41	43.83

Table 1: Top-1 accuracy across ten models in ten datasets. Models are trained and tested on full datasets with their original number of classes (e.g. 1K from ImageNet1K) denoted in the last few digits of the abbreviation of the dataset name. The best score is highlighted in bold while the second best is underlined for each dataset. References for all models and datasets are in the Appendix.
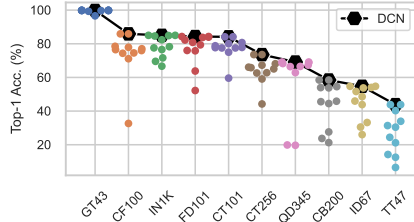
(a) Top-1 accuracy and DCN in ten full datasets.
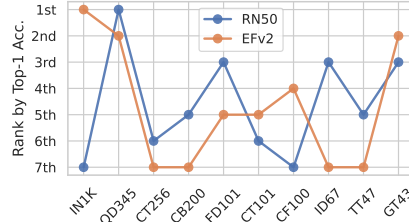
(b) Ranking of ResNet50 (RN50) and EfficientNet V2 (EFv2) across 10 datasets by Top-1 acc.

Figure 2: Many-Class Full Dataset Benchmark.

In the next subsections, we introduce three new types of benchmarks: (1) Few-Class, Full Dataset Trained Benchmark (FC-Full), which benchmarks vision models trained on the full dataset with the original number of classes; (2) Few-Class, Subset Trained Benchmark (FC-Sub), which benchmarks vision models trained on subsets of a fewer number of classes than the full dataset, and (3) Few-Class Similarity Benchmark (FC-Sim), which benchmarks image similarity methods and their correlation with model performance.

3.3 FEW-CLASS FULL DATASET TRAINED BENCHMARK (FC-FULL)

Traditionally, a large number of models are trained and compared on many-class datasets. However, such results cannot be directly transferred to the *Few-Class Regime* and many real-world scenarios. Therefore, we introduce the Few-Class Full Dataset Trained Benchmark (FC-Full), with the objective of effortlessly conducting large-scale experiments and analyses in the *Few-Class Regime*.

The procedure of FC-Full consists of two main stages. In the first stage, users select the models and datasets upon which they would like to conduct experiments. They can choose to download pre-trained model weights, which are usually available on popular model hubs (PyTorch Hub (Foundation, 2024), TensorFlow Hub (Inc., 2024), Hugging Face (Face, 2024), MMPreTrain (Contributors, 2023) etc.). In case of no pre-trained weights available from public websites, users can resort to the option of training from scratch. To that end, our tool is designed and implemented to generate bash scripts for easily configurable and modifiable training through the use of configuration files.

In the second stage, users conduct benchmarking in the *Few-Class Regime*. By specifying the list of classes, *Few-Class Arena* automatically loads pre-trained weights of the chosen models and evaluates performance of the models on the selected datasets. Note that this process is accomplished through configuration files created by the user's specifications, thus enabling hundreds of experiments to be launched by a single command. This dramatically reduces human effort that would otherwise be expended to run these experiments without *Few-Class Arena*.

3.4 FEW-CLASS SUBSET TRAINED BENCHMARK (FC-SUB)

Our study in Figure 1 (red lines) reveals the limits of existing pre-trained models in the *Few-Class Regime*. To facilitate further research and analyze the upper bound performance in the *Few-Class Regime*, we introduce the Few-Class Subset Trained Benchmark (FC-Sub).

FC-Sub follows a similar procedure to FC-Full, except that, when evaluating a model in a subset with a specific number of classes, that model should have been trained on that same subset. Specifically, in Stage One (described for FC-Full), users specify models, datasets and the list of number of classes in configuration files. Then *Few-Class Arena* generates bash scripts for model training on each subset. In Stage two, *Few-Class Arena* tests each model in the same subset that it was trained on.

3.5 FEW-CLASS SIMILARITY BENCHMARK (FC-SIM)

One objective of our tool is to provide the Similarity Benchmark as a platform for researchers to design custom similarity scores for efficient comparison of models and datasets.

The intrinsic image difficulty of a dataset affects a model's classification performance (and human) (Geirhos et al., 2017; Rajalingham et al., 2018; Mayo et al., 2023). We show – as is intuitive – that the more similar two images are, the more difficult it is for a vision classifier to make a correct prediction. This suggests that the level of similarity of images in a dataset can be used as a proxy for a dataset difficulty measure. In this section, we first adopt and provide the basic formulation of similarity, the baseline of a similarity metric. Then we propose a Similarity-Based Silhouette Score to capture the characteristic of image similarity in a dataset.

We first adopt the basic similarity formulation from (Cao et al., 2023). **Intra-Class Similarity** $S_\alpha^{(C)}$ is defined as a scalar describing the similarity of images within a class by taking the average of all the distinct class pairs in C, while **Inter-Class Similarity** denotes a scalar describing the similarity among images in two different classes C_1 and C_2. For a dataset D, these are defined as the mean of their similarity scores over all classes, respectively:

$$S_\alpha^{(D)} = \frac{1}{|L|} \sum_{l \in L} S_\alpha^{(C_l)} = \frac{1}{|L| \times |P^{(C_l)}|} \sum_{l \in L} \sum_{i,j \in C_l;\ i \neq j} \cos(\mathbf{Z}_i, \mathbf{Z}_j), \tag{1}$$

$$S_\beta^{(D)} = \frac{1}{|P^{(D)}|} \sum_{a,b \in L; a \neq b} S_\beta^{(C_a,C_b)} = \frac{1}{|P^{(D)}| \times |P^{(C_1,C_2)}|} \sum_{a,b \in L;\ a \neq b} \sum_{i \in C_1, j \in C_2} \cos(\mathbf{Z}_i, \mathbf{Z}_j). \tag{2}$$

where $|L|$ is the number of classes in a dataset, Z_i is the visual feature of an image i, $|P^{(C)}|$ is the total number of distinct image pairs in class C, $|P^{(D)}|$ is the total number of distinct class pairs, and $|P^{(C_1,C_2)}|$ is the total number of distinct image pairs excluding same-class pairs.

Averaging these similarities provides a single scalar score at the class or dataset level. However, this simplicity neglects other cluster-related information that can better reveal the underlying dataset difficulty property of a dataset. In particular, the **(1) tightness of a class cluster** and **(2) distance to other classes** of class clusters, are features that characterize the inherent class difficulty, but are not captured by S_α or S_β alone.

To compensate the aforementioned drawback, we adopt the Silhouette Score (SS) (Rousseeuw, 1987; Shahapure & Nicholas, 2020): $SS(i) = \frac{b(i)-a(i)}{max(a(i),b(i))}$, where $SS(i)$ is the Silhouette Score of the data point i, $a(i)$ is the average dissimilarity between i and other instances in the same class, and $b(i)$ is the average dissimilarity between i and other data points in the closest different class.

Observe that the above Intra-Class Similarity $S_\alpha^{(C)}$ already represents the tightness of the class (C), therefore $a(i)$ can be replaced with the inverse of Intra-Class Similarity $a(i) = -S_\alpha(i)$. For the

second term $b(i)$, we adopt the previously defined Inter-Class Similarity $S_{\beta}^{(C_1,C_2)}$ and introduce a new similarity score as **Nearest Inter-Class Similarity** $S'^{(C)}_{\beta}$, which is a scalar describing the similarity among instances between class C and the closest class of each instance in C. The dataset-level Nearest Inter-Class Similarity $S'^{(D)}_{\beta}$ is expressed as:

$$S'^{(D)}_{\beta} = \frac{1}{|L|} \sum_{l \in L} S'^{(C_l,\hat{C}_l)}_{\beta} = \frac{1}{|L| \times |P^{(C_l,\hat{C}_l)}|} \sum_{l \in L} \sum_{i \in C_l, j \in \hat{C}_l} \cos(\mathbf{Z}_i, \mathbf{Z}_j). \tag{3}$$

where $\hat{C}$ is the set of the nearest class to C ($\hat{C} \neq C$). To summarize, we introduce our novel **Similarity-Based Silhouette Score** $SimSS$[4]:

$$SimSS^{(D)} = \frac{1}{|L| \times |C_l|} \sum_{i \in C_l} \frac{S_{\alpha}(i) - S'_{\beta}(i)}{max(S_{\alpha}(i), S'_{\beta}(i))}. \tag{4}$$

4 EXPERIMENTAL RESULTS

4.1 RESULTS ON FC-FULL

In this section, we present the results of FC-Full. A model trained on the dataset with its original number of classes (e.g. 1000 in ImageNet1K) is referred to as a *full-class model*. These experiments are designed to understand how full-class model performance changes when the number of classes N_{CL} decreases from many to few classes. We analyze the results of DCN-Full, shown in Figure 3 (details of all models are presented in the Appendix), and we make two key observations when N_{CL} reduces to the *Few-Class Regime* (from right to left). (1) The best performing models do not always increase its accuracy for fewer classes, as shown by the solid red lines that represent the average of DCN for each N_{CL}. (2) The variance, depicted by the light red areas, of the best models broaden dramatically for low N_{CL}, especially for $N_{CL} < 10$.

Both observations support evidence of the limitations of using the common many-class benchmark for application model selection in the *Few-Class Regime*, since it is not consistent between datasets that a model can be made smaller with higher accuracy. Furthermore, the large variance in accuracy means that prediction of performance for few classes is unreliable for this approach.
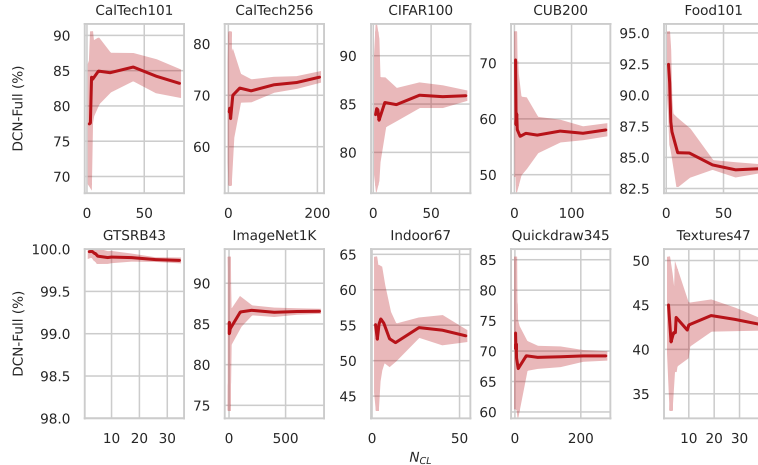

Figure 3: DCN-Full by Top-1 Accuracy (%). N_{CL} ranges from many to 2.

4.2 RESULTS ON FC-SUB

In this section, we show how using *Few-Class Arena* can help reveal more insights in the *Few-Class Regime* to mitigate the issues of Section 4.1.

---

[4]The extended derivation is detailed in the Appendix.

FC-Sub results are displayed in Figure 4. Recall that a *sub-class* model is a model trained on a subset of the dataset where N_{CL} is smaller than the original number of classes in the full dataset. Observe that in the *Few-Class Regime* (when N_{CL} decreases from 4 to 2) that: (1) DCN increases as shown by the solid blue lines, and (2) variance reduces as displayed by the light blue areas.

The preceding observation for FC-Full 4.1 seems to contradict the common belief that, the fewer the classes, the higher is the accuracy that a model can achieve. Conversely, the FC-Sub results do align with this belief. We argue that a full-class model needs to accommodate many parameters to learn features that will enable high performance across all classes in a many-class, full dataset. With the same parameters, however, a sub-class model can adapt to finer and more discriminative features that improve its performance when the number of target classes are much smaller.
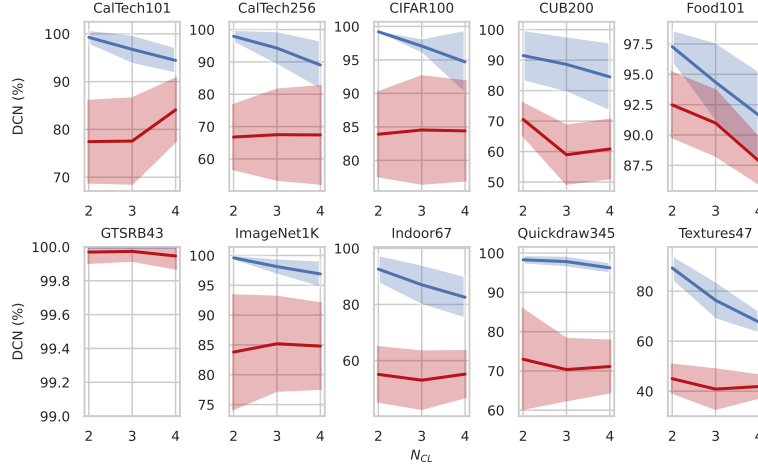

Figure 4: DCN-Sub (red) and DCN-Full (blue) by Top-1 Accuracy (%). N_{CL} ranges from 2 to 4.

4.3 RESULTS ON FC-SIM

In this section, we analyze the use of SimSS (Equation 14) as proxy for few-class dataset difficulty. Experiments are conducted on ImageNet1K using the ResNet family for the lower $N_{CL} \leq 10\%$ range of the original 1000 classes, $N_{CL} \in \{2, 3, 4, 5, 10, 100\}$, and the results are shown in Figure 5. Each datapoint of DCN-Full (diamond in red) or DCN-Sub (square in blue) represents an experiment in a subset of a specific N_{CL}, where classes are sampled from the full dataset. For reproducible results, we use seed numbers from 0 to 4 to generate 5 subsets for one N_{CL} by default. A similarity base function ($sim()$) is defined as the atomic function that takes a pair of images as input and outputs a scalar that represents their image similarity.

In our experiments, we leverage the general visual feature extraction ability of CLIP (image + text) (Radford et al., 2021) and DINOv2 (image) (Oquab et al., 2023) by self-supervised learning. Specifically, a pair of images are fed into its latent space from which the the cosine score is calculated and normalized to 0 to 1. Note that we only use the Image Encoder in CLIP.

Comparing Accuracy and Similarity To evaluate SimSS, we compute the Pearson correlation coefficient (PCC) (r) between model accuracy and SimSS. Results in Figure 5 (a) (b) show that SimSS is poorly correlated with DCN-Full ($r = 0.18$ and $r = 0.26$ for CLIP and DINOv2) due to the large variance shown in Section 4.1 , as well as the general features learned on full-dataset that can be extranious to the target sub-classes. In contrast, SimSS is highly correlated with DCN-Sub (shown in blue squares), with $r = 0.90$ and $r = 0.88$ using CLIP (dashed) and DINOv2 (solid), respectively. We attribute the advantages of DCN-Sub to its focus on the minimal features tailored to the target sub-classes, while maintaining the same number of parameters as the DCN-Full architecture. The high PCC (Wicklin, 2024; Schober et al., 2018) demonstrates that SimSS is a reliable metric to estimate few-class dataset difficulty, and this can help predict the empirical upper-bound accuracy of a model in the *Few-Class Regime*. Comparison between SimSS and all models can be found in the Appendix. Such a high correlation suggests this offers a reliable scaling relationship to estimate model accuracy by similarity for other values of N_{CL} without an exhaustive search. Due to the dataset specificity of the dataset difficulty property, this score is computed once

and used for all times the same dataset is used. We have made available difficulty scores for many datasets at the *Few-Class Arena* site.
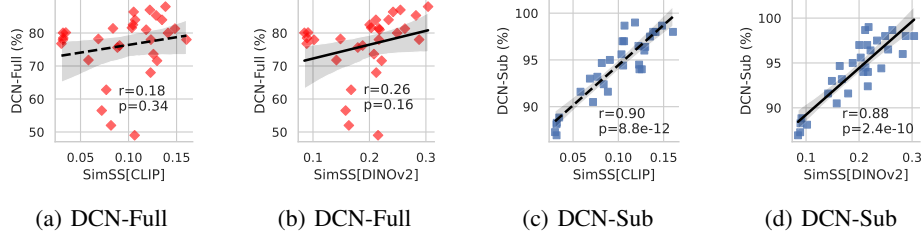

(a) DCN-Full   (b) DCN-Full   (c) DCN-Sub   (d) DCN-Sub

Figure 5: Pearson correlation coefficient (r) between DCN and SimSS when $N_{CL} \in \{2, 3, 4, 5, 10, 100\}$. DCN-Sub (blue squares) is more highly correlated than DCN-Full (red diamonds) with SimSS using both similarity base functions of CLIP (dashed line) and DINOv2 (solid line) with $r \geq 0.88$.

4.4 COMPARISON WITH FINE-TUNED MODELS

Fine-tuning a model from a pre-trained model has become as a common practice in many real-world scenarios. We perform experiments on CNNs (ResNet18, 50) and Transformer architectures (MobileVit-small (Mehta & Rastegari, 2021), ViT-Base) summarized in Table 2. To fine-tune (FT) the ResNet18, 50 and MobileVit-small models for $N_{CL} \in \{2, 4\}$, we first train their full models $N_{CL} = \{100\}$ on CIFAR100 for 100 epochs, and subsequently fine-tune their weights for the target $N_{CL} \in \{2, 4\}$ for another 20 epochs. For ViT, we fine-tune a ViT-B model initialized with weights from the CLIP pre-trained backbone. A linear layer is added on top, and the model is trained for 10 epochs. This setup is indicated by the star symbol (*). We conclude that the fine-tuned models exhibit patterns and trends consistent with the observations presented in Fig. 1. Note our focus of this work is to leverage the proposed difficult measurement method, FC-Sim, to efficiently estimate the achievable model accuracy, thereby assisting in model selection in the *Few-Class Regime*. Sub-models can offer insights into the minimal visual features required for a specific real-world scenario as they are trained exclusively on the target classes. In contrast, weights pre-trained on large full datasets – whether through fully supervised or self-supervised manner – may include extraneous features that are irrelevant to the target classes. We hereby prioritize sub-model study in this work.

MT	N_{CL}	ResNet18	ResNet50	MViT-S	ViT-B
F	100	76.11	73.71	73.83	32.54
F	4	75.10	72.20	72.35	36.15
FT	4	87.60	**90.55**	**90.00**	**91.16***
S	4	**90.65**	90.15	89.45	85.40
F	2	75.00	71.30	71.80	40.80
FT	2	87.90	93.70	90.50	95.20*
S	2	**96.30**	**95.30**	**95.50**	**95.90**

Table 2: Top-1 Accuracies for different configurations on CIFAR100. $N_{CL} \in \{2, 4, 100\}$, MT: Model Type, F: Full model, S: Sub-model, FT: Fine-tuned model, MViT-S: MobileViT-small, *: fine-tuned by the CLIP pre-trained model. Best scores are highlighted in bold. The gray bar indicates sub-models as the primary focus of this research.

5 CONCLUSION

We have proposed *Few-Class Arena* and a dataset difficulty measurement, which together form a benchmark tool to compare and select efficient models in the *Few-Class Regime*. Extensive experiments and analyses over 1500 experiments with 10 models on 10 datasets have helped identify new behavior that is specific to the *Few-Class Regime* as compared to for many-classes. One finding reveals a new N_{CL}-scaling law whereby dataset difficulty must be taken into consideration for accuracy prediction. Such a benchmark will be valuable to the community by providing both researchers and practitioners with a unified framework for future research and real applications.

REFERENCES

P. Lejeune J. Linchant J. Théau A. Delplanque, S. Foucher. Multispecies detection and identification of african mammals in aerial imagery using convolutional neural networks. *Remote Sensing in Ecology and Conservation*, 8(April):166–179, 2022.

SP Arun. Turning visual search time on its head. *Vision Research*, 74:86–92, 2012.

Robert Baldock, Hartmut Maennel, and Behnam Neyshabur. Deep learning through the lens of example difficulty. *Advances in Neural Information Processing Systems*, 34:10876–10889, 2021.

Yonatan Bitton, Nitzan Bitton Guetta, Ron Yosef, Yuval Elovici, Mohit Bansal, Gabriel Stanovsky, and Roy Schwartz. Winogavil: Gamified association benchmark to challenge vision-and-language models. *Advances in Neural Information Processing Systems*, 35:26549–26564, 2022.

Davis Blalock, Jose Javier Gonzalez Ortiz, Jonathan Frankle, and John Guttag. What is the state of neural network pruning? *Proceedings of machine learning and systems*, 2:129–146, 2020.

Lukas Bossard, Matthieu Guillaumin, and Luc Van Gool. Food-101 – mining discriminative components with random forests. In *European Conference on Computer Vision*, 2014.

Yingfeng Cai, Tianyu Luan, Hongbo Gao, Hai Wang, Long Chen, Yicheng Li, Miguel Angel Sotelo, and Zhixiong Li. Yolov4-5d: An effective and efficient object detector for autonomous driving. *IEEE Transactions on Instrumentation and Measurement*, 70:1–13, 2021. doi: 10.1109/TIM. 2021.3065438.

Bryan Bo Cao, Lawrence O'Gorman, Michael Coss, and Shubham Jain. Data-side efficiencies for lightweight convolutional neural networks. *arXiv preprint arXiv:2308.13057*, 2023.

Kai Chen, Jiaqi Wang, Jiangmiao Pang, Yuhang Cao, Yu Xiong, Xiaoxiao Li, Shuyang Sun, Wansen Feng, Ziwei Liu, Jiarui Xu, Zheng Zhang, Dazhi Cheng, Chenchen Zhu, Tianheng Cheng, Qijie Zhao, Buyu Li, Xin Lu, Rui Zhu, Yue Wu, Jifeng Dai, Jingdong Wang, Jianping Shi, Wanli Ouyang, Chen Change Loy, and Dahua Lin. MMDetection: Open mmlab detection toolbox and benchmark. *arXiv preprint arXiv:1906.07155*, 2019.

Ting Chen, Simon Kornblith, Mohammad Norouzi, and Geoffrey Hinton. A simple framework for contrastive learning of visual representations. In *International conference on machine learning*, pp. 1597–1607. PMLR, 2020a.

Xinlei Chen and Kaiming He. Exploring simple siamese representation learning. In *Proceedings of the IEEE/CVF conference on computer vision and pattern recognition*, pp. 15750–15758, 2021.

Xinlei Chen, Haoqi Fan, Ross Girshick, and Kaiming He. Improved baselines with momentum contrastive learning. *arXiv preprint arXiv:2003.04297*, 2020b.

Xinlei Chen, Saining Xie, and Kaiming He. An empirical study of training self-supervised vision transformers. In *Proceedings of the IEEE/CVF international conference on computer vision*, pp. 9640–9649, 2021.

Yu Cheng, Duo Wang, Pan Zhou, and Tao Zhang. A survey of model compression and acceleration for deep neural networks. *arXiv preprint arXiv:1710.09282*, 2017.

M. Cimpoi, S. Maji, I. Kokkinos, S. Mohamed, , and A. Vedaldi. Describing textures in the wild. In *Proceedings of the IEEE Conf. on Computer Vision and Pattern Recognition (CVPR)*, 2014.

MMPreTrain Contributors. Openmmlab's pre-training toolbox and benchmark. https://github.com/open-mmlab/mmpretrain, 2023.

Jia Deng, Wei Dong, Richard Socher, Li-Jia Li, Kai Li, and Li Fei-Fei. Imagenet: A large-scale hierarchical image database. In *2009 IEEE conference on computer vision and pattern recognition*, pp. 248–255. Ieee, 2009.

Xiaohan Ding, X. Zhang, Ningning Ma, Jungong Han, Guiguang Ding, and Jian Sun. Repvgg: Making vgg-style convnets great again. *2021 IEEE/CVF Conference on Computer Vision and Pattern Recognition (CVPR)*, pp. 13728–13737, 2021. URL https://api.semanticscholar.org/CorpusID:231572790.

Alexey Dosovitskiy, Lucas Beyer, Alexander Kolesnikov, Dirk Weissenborn, Xiaohua Zhai, Thomas Unterthiner, Mostafa Dehghani, Matthias Minderer, Georg Heigold, Sylvain Gelly, et al. An image is worth 16x16 words: Transformers for image recognition at scale. *arXiv preprint arXiv:2010.11929*, 2020.

DC Dowson and BV666017 Landau. The fréchet distance between multivariate normal distributions. *Journal of multivariate analysis*, 12(3):450–455, 1982.

Hugging Face. Hugging face models. https://huggingface.co/models, 2024. URL https://huggingface.co/models. Accessed on 2024-06-04.

Alex Fang, Simon Kornblith, and Ludwig Schmidt. Does progress on imagenet transfer to real-world datasets? *Advances in Neural Information Processing Systems*, 36, 2024.

The Linux Foundation. Pytorch hub. https://pytorch.org/hub, 2024. URL https://pytorch.org/hub. Accessed on 2024-06-04.

Robert Geirhos, David HJ Janssen, Heiko H Sch"utt, Jonas Rauber, Matthias Bethge, and Felix A Wichmann. Comparing deep neural networks against humans: object recognition when the signal gets weaker. *arXiv preprint arXiv:1706.06969*, 2017.

Micah Goldblum, Hossein Souri, Renkun Ni, Manli Shu, Viraj Prabhu, Gowthami Somepalli, Prithvijit Chattopadhyay, Mark Ibrahim, Adrien Bardes, Judy Hoffman, et al. Battle of the backbones: A large-scale comparison of pretrained models across computer vision tasks. *Advances in Neural Information Processing Systems*, 36, 2024.

Ian J Goodfellow, Jonathon Shlens, and Christian Szegedy. Explaining and harnessing adversarial examples. *arXiv preprint arXiv:1412.6572*, 2014.

Gregory Griffin, Alex Holub, and Pietro Perona. Caltech 256, Apr 2022.

Philipp Gysel, Jon Pimentel, Mohammad Motamedi, and Soheil Ghiasi. Ristretto: A framework for empirical study of resource-efficient inference in convolutional neural networks. *IEEE transactions on neural networks and learning systems*, 29(11):5784–5789, 2018.

David Ha and Douglas Eck. A neural representation of sketch drawings. *arXiv preprint arXiv:1704.03477*, 2017.

Song Han, Huizi Mao, and William J Dally. Deep compression: Compressing deep neural networks with pruning, trained quantization and huffman coding. *arXiv preprint arXiv:1510.00149*, 2015.

Kaiming He, Xiangyu Zhang, Shaoqing Ren, and Jian Sun. Deep residual learning for image recognition. In *Proceedings of the IEEE conference on computer vision and pattern recognition*, pp. 770–778, 2016.

Kaiming He, Haoqi Fan, Yuxin Wu, Saining Xie, and Ross Girshick. Momentum contrast for unsupervised visual representation learning. In *Proceedings of the IEEE/CVF conference on computer vision and pattern recognition*, pp. 9729–9738, 2020.

Kaiming He, Xinlei Chen, Saining Xie, Yanghao Li, Piotr Dollár, and Ross Girshick. Masked autoencoders are scalable vision learners. In *Proceedings of the IEEE/CVF conference on computer vision and pattern recognition*, pp. 16000–16009, 2022.

Martin Heusel, Hubert Ramsauer, Thomas Unterthiner, Bernhard Nessler, and Sepp Hochreiter. Gans trained by a two time-scale update rule converge to a local nash equilibrium. *Advances in neural information processing systems*, 30, 2017.

Alain Hore and Djemel Ziou. Image quality metrics: Psnr vs. ssim. In *2010 20th international conference on pattern recognition*, pp. 2366–2369. IEEE, 2010.

Andrew Howard, Mark Sandler, Grace Chu, Liang-Chieh Chen, Bo Chen, Mingxing Tan, Weijun Wang, Yukun Zhu, Ruoming Pang, Vijay Vasudevan, et al. Searching for mobilenetv3. In *Proceedings of the IEEE/CVF international conference on computer vision*, pp. 1314–1324, 2019.

Shell Xu Hu, Da Li, Jan St"uhmer, Minyoung Kim, and Timothy M Hospedales. Pushing the limits of simple pipelines for few-shot learning: External data and fine-tuning make a difference. In *Proceedings of the IEEE/CVF Conference on Computer Vision and Pattern Recognition*, pp. 9068–9077, 2022.

Forrest N Iandola, Song Han, Matthew W Moskewicz, Khalid Ashraf, William J Dally, and Kurt Keutzer. Squeezenet: Alexnet-level accuracy with 50x fewer parameters and¡ 0.5 mb model size. *arXiv preprint arXiv:1602.07360*, 2016.

Google Inc. Tensorflow hub. https://www.tensorflow.org/hub, 2024. URL https://www.tensorflow.org/hub. Accessed on 2024-06-04.

Ashish Jaiswal, Ashwin Ramesh Babu, Mohammad Zaki Zadeh, Debapriya Banerjee, and Fillia Makedon. A survey on contrastive self-supervised learning. *Technologies*, 9(1):2, 2020.

Ziheng Jiang, Chiyuan Zhang, Kunal Talwar, and Michael C Mozer. Characterizing structural regularities of labeled data in overparameterized models. *arXiv preprint arXiv:2002.03206*, 2020.

Longlong Jing and Yingli Tian. Self-supervised visual feature learning with deep neural networks: A survey. *IEEE transactions on pattern analysis and machine intelligence*, 43(11):4037–4058, 2020.

Jared Kaplan, Sam McCandlish, Tom Henighan, Tom B Brown, Benjamin Chess, Rewon Child, Scott Gray, Alec Radford, Jeffrey Wu, and Dario Amodei. Scaling laws for neural language models. *arXiv preprint arXiv:2001.08361*, 2020.

Kohitij Kar, Jonas Kubilius, Kailyn Schmidt, Elias B Issa, and James J DiCarlo. Evidence that recurrent circuits are critical to the ventral stream's execution of core object recognition behavior. *Nature neuroscience*, 22(6):974–983, 2019.

Alex Krizhevsky, Geoffrey Hinton, et al. Learning multiple layers of features from tiny images. 2009.

Manoj Kumar, Neil Houlsby, Nal Kalchbrenner, and Ekin D Cubuk. Do better imagenet classifiers assess perceptual similarity better? *arXiv preprint arXiv:2203.04946*, 2022.

Hugo Laurençon, Lucile Saulnier, Léo Tronchon, Stas Bekman, Amanpreet Singh, Anton Lozhkov, Thomas Wang, Siddharth Karamcheti, Alexander Rush, Douwe Kiela, et al. Obelics: An open web-scale filtered dataset of interleaved image-text documents. *Advances in Neural Information Processing Systems*, 36, 2024.

Tiep Le, Vasudev Lal, and Phillip Howard. Coco-counterfactuals: Automatically constructed counterfactual examples for image-text pairs. *Advances in Neural Information Processing Systems*, 36, 2024.

Tony Lee, Michihiro Yasunaga, Chenlin Meng, Yifan Mai, Joon Sung Park, Agrim Gupta, Yunzhi Zhang, Deepak Narayanan, Hannah Teufel, Marco Bellagente, et al. Holistic evaluation of text-to-image models. *Advances in Neural Information Processing Systems*, 36, 2024.

Cong Leng, Zesheng Dou, Hao Li, Shenghuo Zhu, and Rong Jin. Extremely low bit neural network: Squeeze the last bit out with admm. In *Proceedings of the AAAI conference on artificial intelligence*, volume 32, 2018.

Fei-Fei Li, Marco Andreeto, Marc'Aurelio Ranzato, and Pietro Perona. Caltech 101, Apr 2022a.

Hao Li, Asim Kadav, Igor Durdanovic, Hanan Samet, and Hans Peter Graf. Pruning filters for efficient convnets. *arXiv preprint arXiv:1608.08710*, 2016.

Yanyu Li, Geng Yuan, Yang Wen, Eric Hu, Georgios Evangelidis, S. Tulyakov, Yanzhi Wang, and Jian Ren. Efficientformer: Vision transformers at mobilenet speed. *ArXiv*, abs/2206.01191, 2022b. URL https://api.semanticscholar.org/CorpusID:249282517.

Tsung-Yi Lin, Michael Maire, Serge Belongie, James Hays, Pietro Perona, Deva Ramanan, Piotr Dollár, and C Lawrence Zitnick. Microsoft coco: Common objects in context. In *European conference on computer vision*, pp. 740–755. Springer, 2014.

Ze Liu, Yutong Lin, Yue Cao, Han Hu, Yixuan Wei, Zheng Zhang, Stephen Lin, and Baining Guo. Swin transformer: Hierarchical vision transformer using shifted windows. *2021 IEEE/CVF International Conference on Computer Vision (ICCV)*, pp. 9992–10002, 2021. URL https://api.semanticscholar.org/CorpusID:232352874.

Ze Liu, Han Hu, Yutong Lin, Zhuliang Yao, Zhenda Xie, Yixuan Wei, Jia Ning, Yue Cao, Zheng Zhang, Li Dong, et al. Swin transformer v2: Scaling up capacity and resolution. In *Proceedings of the IEEE/CVF conference on computer vision and pattern recognition*, pp. 12009–12019, 2022a.

Zhuang Liu, Hanzi Mao, Chaozheng Wu, Christoph Feichtenhofer, Trevor Darrell, and Saining Xie. A convnet for the 2020s. *2022 IEEE/CVF Conference on Computer Vision and Pattern Recognition (CVPR)*, pp. 11966–11976, 2022b. URL https://api.semanticscholar.org/CorpusID:245837420.

Mario Lucic, Karol Kurach, Marcin Michalski, Sylvain Gelly, and Olivier Bousquet. Are gans created equal? a large-scale study. *Advances in neural information processing systems*, 31, 2018.

Ningning Ma, Xiangyu Zhang, Hai-Tao Zheng, and Jian Sun. Shufflenet v2: Practical guidelines for efficient cnn architecture design. In *Proceedings of the European conference on computer vision (ECCV)*, pp. 116–131, 2018.

David Mayo, Jesse Cummings, Xinyu Lin, Dan Gutfreund, Boris Katz, and Andrei Barbu. How hard are computer vision datasets? calibrating dataset difficulty to viewing time. *Advances in Neural Information Processing Systems*, 36:11008–11036, 2023.

S Mehta and M Rastegari. Mobilevit: Light-weight, general-purpose, and mobile-friendly vision transformer. arxiv 2021. *arXiv preprint arXiv:2110.02178*.

Sachin Mehta and Mohammad Rastegari. Mobilevit: light-weight, general-purpose, and mobile-friendly vision transformer. *arXiv preprint arXiv:2110.02178*, 2021.

Maxime Oquab, Timothée Darcet, Théo Moutakanni, Huy Vo, Marc Szafraniec, Vasil Khalidov, Pierre Fernandez, Daniel Haziza, Francisco Massa, Alaaeldin El-Nouby, et al. Dinov2: Learning robust visual features without supervision. *arXiv preprint arXiv:2304.07193*, 2023.

David Patterson, Joseph Gonzalez, Quoc Le, Chen Liang, Lluis-Miquel Munguia, Daniel Rothchild, David So, Maud Texier, and Jeff Dean. Carbon emissions and large neural network training. *arXiv preprint arXiv:2104.10350*, 2021.

Zhiliang Peng, Wei Huang, Shanzhi Gu, Lingxi Xie, Yaowei Wang, Jianbin Jiao, and Qixiang Ye. Conformer: Local features coupling global representations for visual recognition. *2021 IEEE/CVF International Conference on Computer Vision (ICCV)*, pp. 357–366, 2021. URL https://api.semanticscholar.org/CorpusID:234338988.

Ariadna Quattoni and Antonio Torralba. Recognizing indoor scenes. In *2009 IEEE conference on computer vision and pattern recognition*, pp. 413–420. IEEE, 2009.

Alec Radford, Jong Wook Kim, Chris Hallacy, Aditya Ramesh, Gabriel Goh, Sandhini Agarwal, Girish Sastry, Amanda Askell, Pamela Mishkin, Jack Clark, et al. Learning transferable visual models from natural language supervision. In *International conference on machine learning*, pp. 8748–8763. PMLR, 2021.

Jack W Rae, Sebastian Borgeaud, Trevor Cai, Katie Millican, Jordan Hoffmann, Francis Song, John Aslanides, Sarah Henderson, Roman Ring, Susannah Young, et al. Scaling language models: Methods, analysis & insights from training gopher. *arXiv preprint arXiv:2112.11446*, 2021.

Rishi Rajalingham, Elias B Issa, Pouya Bashivan, Kohitij Kar, Kailyn Schmidt, and James J DiCarlo. Large-scale, high-resolution comparison of the core visual object recognition behavior of humans, monkeys, and state-of-the-art deep artificial neural networks. *Journal of Neuroscience*, 38(33): 7255–7269, 2018.

Peter J Rousseeuw. Silhouettes: a graphical aid to the interpretation and validation of cluster analysis. *Journal of computational and applied mathematics*, 20:53–65, 1987.

Mark Sandler, Andrew Howard, Menglong Zhu, Andrey Zhmoginov, and Liang-Chieh Chen. Mobilenetv2: Inverted residuals and linear bottlenecks. In *Proceedings of the IEEE conference on computer vision and pattern recognition*, pp. 4510–4520, 2018.

Florian Scheidegger, Luca Benini, Costas Bekas, and A Cristiano I Malossi. Constrained deep neural network architecture search for iot devices accounting for hardware calibration. *Advances in Neural Information Processing Systems*, 32, 2019.

Florian Scheidegger, Roxana Istrate, Giovanni Mariani, Luca Benini, Costas Bekas, and Cristiano Malossi. Efficient image dataset classification difficulty estimation for predicting deep-learning accuracy. *The Visual Computer*, 37(6):1593–1610, 2021.

Patrick Schober, Christa Boer, and Lothar A Schwarte. Correlation coefficients: appropriate use and interpretation. *Anesthesia & analgesia*, 126(5):1763–1768, 2018.

Ketan Rajshekhar Shahapure and Charles Nicholas. Cluster quality analysis using silhouette score. In *2020 IEEE 7th international conference on data science and advanced analytics (DSAA)*, pp. 747–748. IEEE, 2020.

Zhenfeng Shao, Linggang Wang, Zhongyuan Wang, Wan Du, and Wenjing Wu. Saliency-aware convolution neural network for ship detection in surveillance video. *IEEE Transactions on Circuits and Systems for Video Technology*, 30(3):781–794, 2020.

Hamid R Sheikh and Alan C Bovik. Image information and visual quality. *IEEE Transactions on image processing*, 15(2):430–444, 2006.

Maying Shen, Hongxu Yin, Pavlo Molchanov, Lei Mao, Jianna Liu, and Jose M Alvarez. Structural pruning via latency-saliency knapsack. *arXiv preprint arXiv:2210.06659*, 2022.

Karen Simonyan and Andrew Zisserman. Very deep convolutional networks for large-scale image recognition. *CoRR*, abs/1409.1556, 2014a. URL https://api.semanticscholar.org/CorpusID:14124313.

Karen Simonyan and Andrew Zisserman. Very deep convolutional networks for large-scale image recognition. *arXiv preprint arXiv:1409.1556*, 2014b.

Debjyoti Sinha and Mohamed El-Sharkawy. Thin mobilenet: An enhanced mobilenet architecture. In *2019 IEEE 10th annual ubiquitous computing, electronics & mobile communication conference (UEMCON)*, pp. 0280–0285. IEEE, 2019.

Yisheng Song, Ting Wang, Puyu Cai, Subrota K Mondal, and Jyoti Prakash Sahoo. A comprehensive survey of few-shot learning: Evolution, applications, challenges, and opportunities. *ACM Computing Surveys*, 55(13s):1–40, 2023.

J. Stallkamp, M. Schlipsing, J. Salmen, and C. Igel. Man vs. computer: Benchmarking machine learning algorithms for traffic sign recognition. *Neural Networks*, (0):–, 2012. ISSN 0893-6080. doi: 10.1016/j.neunet.2012.02.016. URL http://www.sciencedirect.com/science/article/pii/S0893608012000457.

Flood Sung, Yongxin Yang, Li Zhang, Tao Xiang, Philip HS Torr, and Timothy M Hospedales. Learning to compare: Relation network for few-shot learning. In *Proceedings of the IEEE conference on computer vision and pattern recognition*, pp. 1199–1208, 2018.

Christian Szegedy, Vincent Vanhoucke, Sergey Ioffe, Jon Shlens, and Zbigniew Wojna. Rethinking the inception architecture for computer vision. In *Proceedings of the IEEE conference on computer vision and pattern recognition*, pp. 2818–2826, 2016.

M. Tan and Q. L. Efficientnetv2: Smaller models and faster training. In *International conference on machine learning*, pp. 10096–10106. PMLR, 2021.

Mingxing Tan and Quoc Le. Efficientnet: Rethinking model scaling for convolutional neural networks. In *International conference on machine learning*, pp. 6105–6114. PMLR, 2019a.

Mingxing Tan and Quoc V. Le. Efficientnet: Rethinking model scaling for convolutional neural networks. *ArXiv*, abs/1905.11946, 2019b. URL `https://api.semanticscholar.org/CorpusID:167217261`.

Lana M Trick and James T Enns. Lifespan changes in attention: The visual search task. *Cognitive Development*, 13(3):369–386, 1998.

Radu Tudor Ionescu, Bogdan Alexe, Marius Leordeanu, Marius Popescu, Dim P Papadopoulos, and Vittorio Ferrari. How hard can it be? estimating the difficulty of visual search in an image. In *Proceedings of the IEEE Conference on Computer Vision and Pattern Recognition*, pp. 2157–2166, 2016.

Catherine Wah, Steve Branson, Peter Welinder, Pietro Perona, and Serge Belongie. *The Caltech-UCSD Birds-200-2011 Dataset*. Jul 2011.

Jiang Wang, Yang Song, Thomas Leung, Chuck Rosenberg, Jingbin Wang, James Philbin, Bo Chen, and Ying Wu. Learning fine-grained image similarity with deep ranking. In *Proceedings of the IEEE conference on computer vision and pattern recognition*, pp. 1386–1393, 2014.

Yaqing Wang, Quanming Yao, James T Kwok, and Lionel M Ni. Generalizing from a few examples: A survey on few-shot learning. *ACM computing surveys (csur)*, 53(3):1–34, 2020.

Zhou Wang, Alan C Bovik, Hamid R Sheikh, and Eero P Simoncelli. Image quality assessment: from error visibility to structural similarity. *IEEE transactions on image processing*, 13(4):600–612, 2004.

Rick Wicklin. Weak or strong? how to interpret a spearman or kendall correlation. `https://blogs.sas.com/content/iml/2023/04/05/interpret-spearman-kendall-corr.html`, 2024. URL `https://blogs.sas.com/content/iml/2023/04/05/interpret-spearman-kendall-corr.html`. Accessed on 2024-06-04.

Jeremy M Wolfe, Evan M Palmer, and Todd S Horowitz. Reaction time distributions constrain models of visual search. *Vision research*, 50(14):1304–1311, 2010.

Sanghyun Woo, Shoubhik Debnath, Ronghang Hu, Xinlei Chen, Zhuang Liu, In So Kweon, and Saining Xie. Convnext v2: Co-designing and scaling convnets with masked autoencoders. In *Proceedings of the IEEE/CVF Conference on Computer Vision and Pattern Recognition*, pp. 16133–16142, 2023.

Serena Yeung, Olga Russakovsky, Greg Mori, and Li Fei-Fei. End-to-end learning of action detection from frame glimpses in videos. In *Proceedings of the IEEE conference on computer vision and pattern recognition*, pp. 2678–2687, 2016.

Xiaohua Zhai, Alexander Kolesnikov, Neil Houlsby, and Lucas Beyer. Scaling vision transformers. In *Proceedings of the IEEE/CVF conference on computer vision and pattern recognition*, pp. 12104–12113, 2022.

Dengsheng Zhang and Guojun Lu. Evaluation of similarity measurement for image retrieval. In *International conference on neural networks and signal processing, 2003. proceedings of the 2003*, volume 2, pp. 928–931. IEEE, 2003.

Xiangyu Zhang, Xinyu Zhou, Mengxiao Lin, and Jian Sun. Shufflenet: An extremely efficient convolutional neural network for mobile devices. *2018 IEEE/CVF Conference on Computer Vision and Pattern Recognition*, pp. 6848–6856, 2017. URL `https://api.semanticscholar.org/CorpusID:24982157`.

A Appendix

A.1 Goals

1. Generality. All vision models and existing datasets for classification should be compatible in this framework. In addition, users can extend to custom models and datasets for their needs.

2. Efficiency. The benchmark should be time- and space-efficient for users. The experimental setup for the few-class benchmark should be easily specified by a few hyper-parameters (e.g. number of classes). Since the few-class regime usually includes sub-datasets extracted from the full dataset, the benchmark should be able to locate those sub-datasets without generating redundant duplicates for reasons of storage efficiency. For time-efficiency, it should conduct training and testing automatically through use of user-specified configuration files, without users' manual execution.

3. Large-Scale Benchmark. The tool should allow for large-scale benchmarking, including training and testing of different vision models on various datasets when the number of classes varies.

A.2 Benchmark Usage Guideline

Users should prepare the dataset detailed in 3.1 in the "CUSTOM" format based on the MMPreTrain (Contributors, 2023) documentation. The tool is designed for both practitioners and researchers.

Practitioner: Users select the target N_{CL} and then execute the FC-Sim on the custom dataset. FC-Sim calculates the image similarity score which can be used to index a narrow range of potential target models, given the deployment accuracy requirement (e.g. accuracy). We provide the index table covering ten models on ten datasets for the *Few-Class Regime*.

Researcher: Users specify the configurations for FC-Full, FC-Sub and FC-Sim, as well as a list of N_{CL}. In the next step, users can execute the scripts running on all benchmarks on the custom dataset. The results for all benchmarks are then used for further analysis.

A.3 Extended Related Work

Few-Shot Learning. There has been a large body of research on Few-Short Learning (FSL) (Song et al., 2023; Wang et al., 2020; Hu et al., 2022; Sung et al., 2018). However, the fundamental research questions differ from ours in the *Few-Class Regime*. The FSL framework aims to address the problem of **data scarsity** with the goal for a model to leverage the representations from very few samples (or none, in the case of Zero-Shot Learning), or prior knowledge that can **generalize** effectively to other tasks or domains.

Self-Supervised Learning. To leverage the knowledge from unlabled data, Self-Supervised Learning (SSL) has emerged as an effective learning framework to learn general vision features (Jaiswal et al., 2020; Jing & Tian, 2020). This includes techniques such as Contrastive Learning, applied to single modalities (Chen et al., 2020a; Chen & He, 2021; He et al., 2020; Chen et al., 2020b; 2021) or multiple modalities (Radford et al., 2021), as well as mask-and-reconstruct methods (He et al., 2022), among others.

In contrast to the advancements of the aforementioned learning frameworks, *Few-Class Arena* focuses on the research problem of selecting the most **efficient** model with **minimal** features needed for the target application deployment.

A.4 Full Models on ImageNet

In practice, ImageNet serves as a common benchmark for vision neural networks. We list the details of 10 pre-trained models from MMPreTrain (Contributors, 2023) in terms of Top-1 Accuracy and scale ($\#Params$) in Fig. 6.
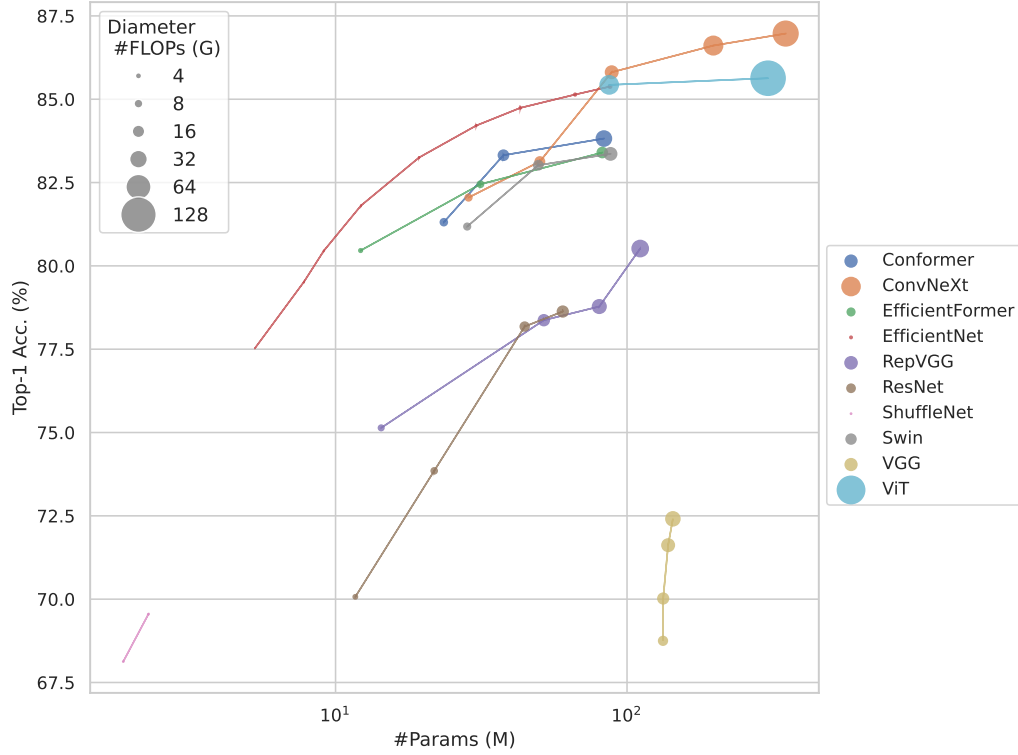
Figure 6: Top-1 Accuracy (%) vs. number of parameters and FLOPs (G) (size of circle) on ImageNet.

Model	Ref.	Model	Ref.
Conformer	(Peng et al., 2021)	ConvNeXt	(Liu et al., 2022b)
EfficientFormer	(Li et al., 2022b)	EfficientNet	(Tan & Le, 2019b)
RepVGG	(Ding et al., 2021)	ResNet	(He et al., 2016)
ShuffleNet	(Zhang et al., 2017)	Swin	(Liu et al., 2021)
VGG	(Simonyan & Zisserman, 2014a)	ViT	(Dosovitskiy et al., 2020)

Table 3: Full models pre-trained on ImageNet.

A.5 EXTENDED MANY-CLASS FULL DATASET TRAINED BENCHMARK RESULTS

A complete ranking of 10 models in 10 datasets is depicted in Fig. 7. Observe that the 10 models' rankings differ dramatically among 10 different datasets where each line changes from ImageNet1K (IN1K) to other datasets. This poses some questions whether rankings in existing benchmarks can be a reliable indicator for a practitioner to select an efficient neural network, especially when the deployed environment changes from application to application. A major variable in this process is the reduced number of classes from benchmark datasets to deployed environments in the *Few-Class Regime*. As such, our tool is developed to facilitate research in the *Few-Class Regime*.
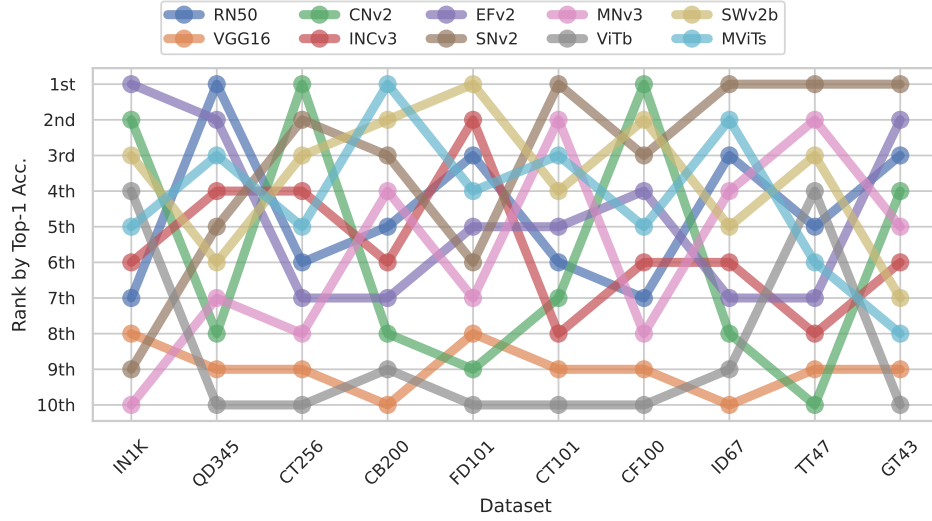
17

Figure 7: Extended Details of Fig. 2 (b) in the main paper. Full Ranking of 10 models across 10 datasets by Top-1 acc.

A.6 DATASETS

Dataset information is presented in Table 4.

Dataset Name	Abbrev.	Ref.	Homepage	Path in FCA
Caltech 101	CT101	(Li et al., 2022a)	data.caltech.edu/records/mzrjq-6wc02	tools/ncls/datasets/caltech101.py
Caltech 256	CT256	(Griffin et al., 2022)	data.caltech.edu/records/nyy15-4j048	tools/ncls/datasets/caltech256.py
CIFAR-100	CF100	(Krizhevsky et al., 2009)	cs.toronto.edu/ kriz/cifar.html github.com/knjcode/cifar2png	tools/ncls/datasets/cifar100.py
Caltech-UCSD Birds-200-2011	CB200	(Wah et al., 2011)	vision.caltech.edu/visipedia/CUB-200-2011.html data.caltech.edu/records/65de6-vp158/files/CUB_200_2011.tgz	tools/ncls/datasets/cub200.py
Food 101	FD101	(Bossard et al., 2014)	vision.ee.ethz.ch/datasets_extra/food-101/ huggingface.co/datasets/food101	tools/ncls/datasets/food101.py
German Traffic Sign	GT43	(Stallkamp et al., 2012)	benchmark.ini.rub.de/	tools/ncls/datasets/gtsrb43.py
ImageNet	IN1K	(Deng et al., 2009)	image-net.org/challenges/LSVRC/2012/index.php	*
Indoor Scene Recognition	ID67	(Quattoni & Torralba, 2009)	web.mit.edu/torralba/www/indoor.html	tools/ncls/datasets/indoor67.py
Quickdraw	QD345	(Ha & Eck, 2017)	github.com/googlecreativelab/quickdraw-dataset tensorflow.org/datasets/community_catalog/huggingface/quickdraw	tools/ncls/datasets/quickdraw345.py
Describable Textures Dataset	TT47	(Cimpoi et al., 2014)	robots.ox.ac.uk/ vgg/data/dtd/index.html	tools/ncls/datasets/textures47.py

Table 4: Dataset information. * Note that ImageNet dataset format is used as the reference for other datasets. Therefore Path in FCA for ImageNet is not required.

License. We have searched available online resources and list the license of each dataset in Table 5. For licenses not found in the datasets or websites denoted as "*", we assume they are non-commercial research use only.

18

Dataset	License	Dataset	License
CT101	CC BY 4.0	CT256	CC BY 4.0
CF100	*	CB200	*
FD101	*	GT43	*
IN1K	*	ID67	(DbCL) v1.0
QD345	CC BY 4.0	TT47	*

Table 5: Licenses of ten datasets.

Train/val splits. The dataset format follows the convention of ImageNet:

```
imagenet1k/
    meta
        train.txt
        val.txt
    train
        <IMAGE_ID>.jpeg
        ...
    val
        <IMAGE_ID>.jpeg
        ...
```

where a .txt file stores a pair of image id and and class number in each row in the following format

```
<IMAGE_ID>.jpeg <CLASS_NUM>
```

We follow the same train/val splits when the original dataset has already provided. If the dataset does not have explicit splits, we first assign image IDs to all images, starting from 0, and select $4/5$ of all images as training set and put the rest in the validation set. Specifially, when an image whose ID satisfies the condition $ID \% 5 == 0$, it will be moved to the validation set. Otherwise, it will be assigned as a training sample.

A.7 MODEL TRAINING DETAILS

Model training details are presented in Table 6.

Model	Abbrev.	Ref.	Optimizer	LR	Weight Decay	Other Params
ResNet50	RN50	(He et al., 2016)	SGD	0.1	1e-4	momentum=0.9
VGG16	VGG16	(Simonyan & Zisserman, 2014b)	SGD	0.01	1e-4	momentum=0.9
ConvNeXt V2 Base	CNv2	(Woo et al., 2023)	AdamW	2.5e-3	0.05	eps=1e-8 betas=(0.9, 0.999)
Inception V3	INCv3	(Szegedy et al., 2016)	SGD	0.1	1e-4	momentum=0.9
EfficientNet V2 Medium	EFv2	(Tan & L., 2021)	SGD	4e-3	0.1	momentum=0.9 clip_grad: max_norm=5.0
ShuffleNet V2	SNv2	(Ma et al., 2018)	SGD	0.5	0.9	momentum=4e-5
MobileNet V3 Small	MNv3	(Howard et al., 2019)	RMSprop	6.4e-4	1e-5	alpha=0.9 momentum=0.9 eps=0.0316
Vision Transformer Base	ViTb	(Dosovitskiy et al., 2020)	AdamW	3e-3	0.3	-
Swin Transformer V2 Base	SWv2b	(Liu et al., 2022a)	AdamW	1e-4	0.05	eps=1e-8 betas=(0.9, 0.999)
MobileViT Small	MViTs	(Mehta & Rastegari)	SGD	0.1	1e-4	momentum=0.9

Table 6: Model Training information. LR: Learning rate. SGD: Stochastic gradient descent. AdamW: Adam with weight decay. RMSprop: Root mean square propagation.

A.8 EXTENDED FEW-CLASS FULL DATASET TRAINED BENCHMARK (FC-FULL) RESULTS

We present the details of FC-Full results for each experiment model, including ResNet50, VGG16, ConNeXt V2 Base, Inception V3, EfficientNet V2 Medium, ShuffleNet V2, MobileNet V3 Small, ViT Base, Swin Transformer V2 Base, MobileViT Small in Fig. 8-17, respectively.
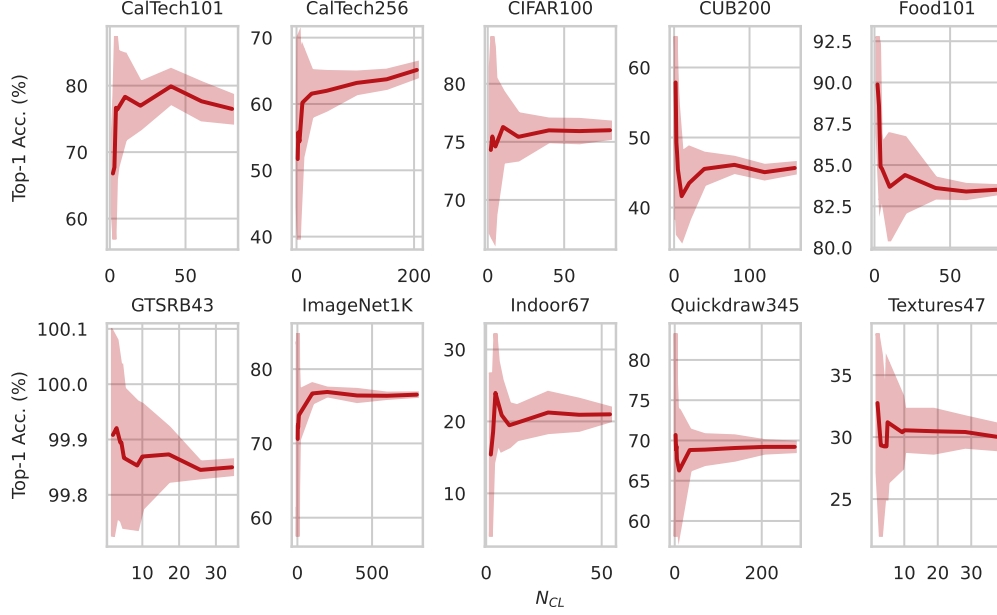
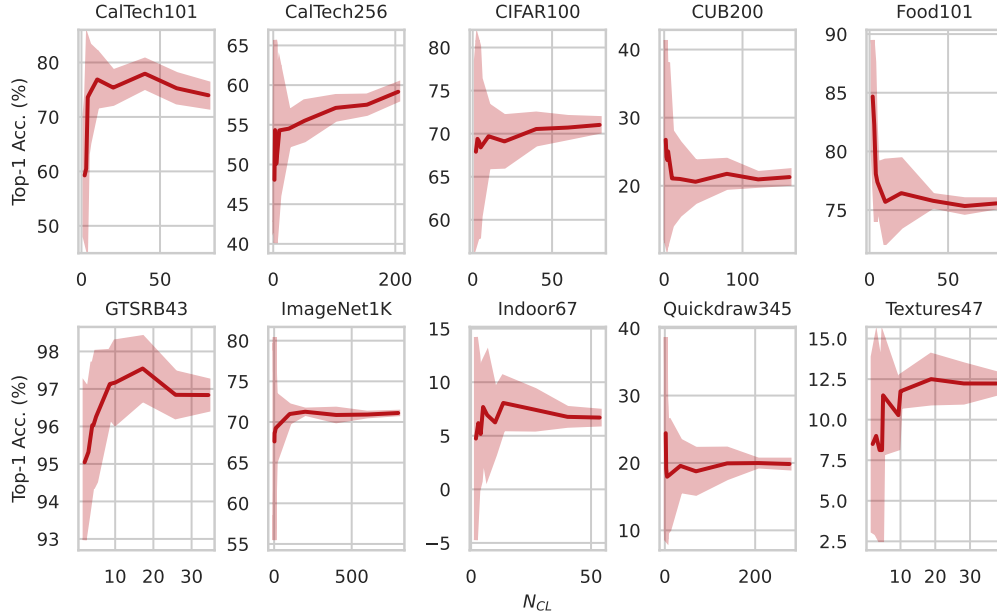Figure 8: FC-Full Top-1 Accuracy (%) for ResNet50.
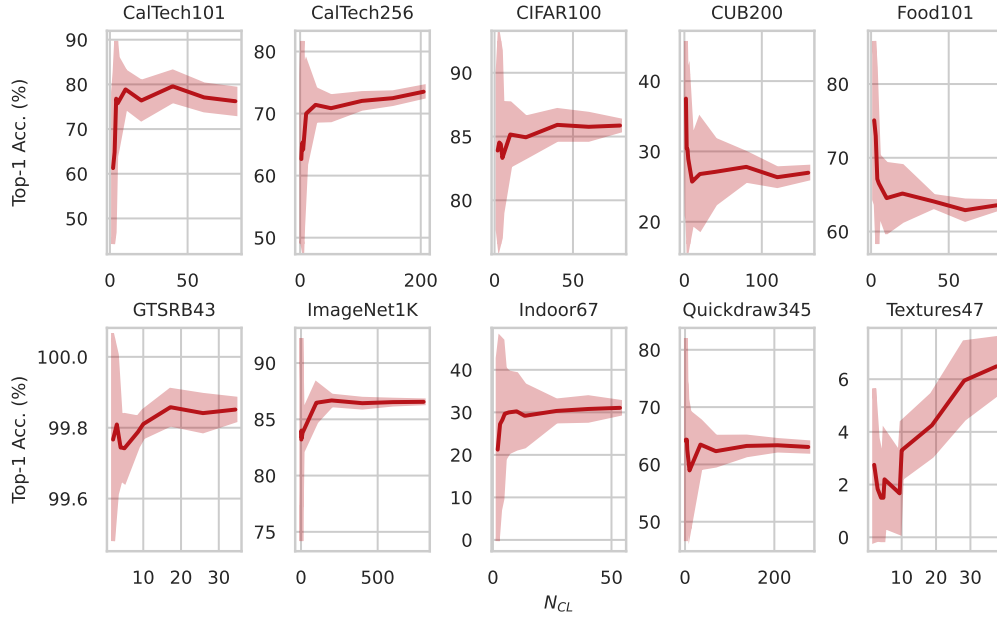
Figure 9: FC-Full Top-1 Accuracy (%) for VGG16.
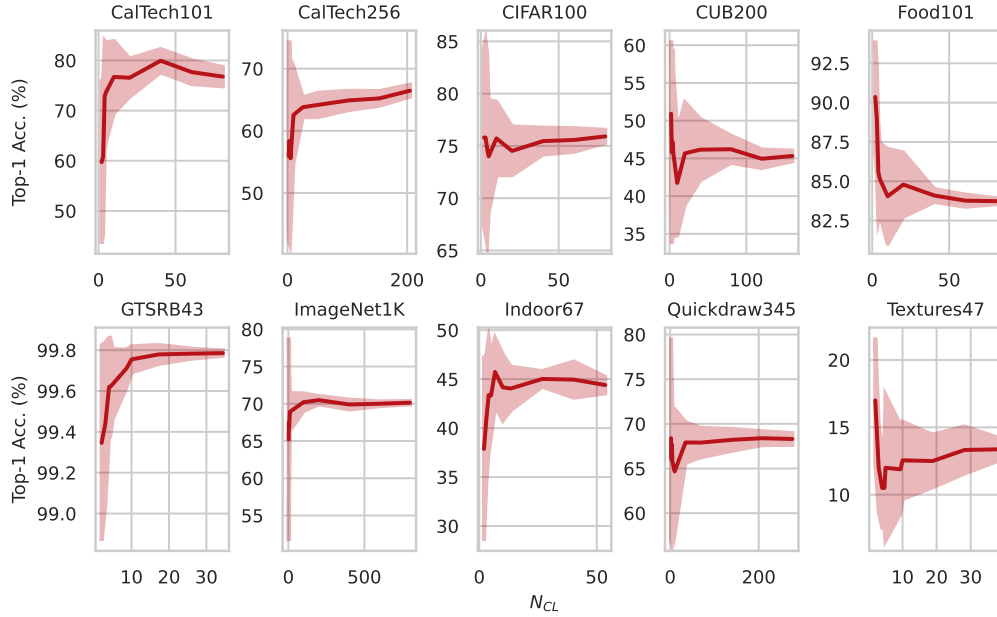
Figure 10: FC-Full Top-1 Accuracy (%) for ConNeXt V2 Base.

Figure 11: FC-Full Top-1 Accuracy (%) for Inception V3.
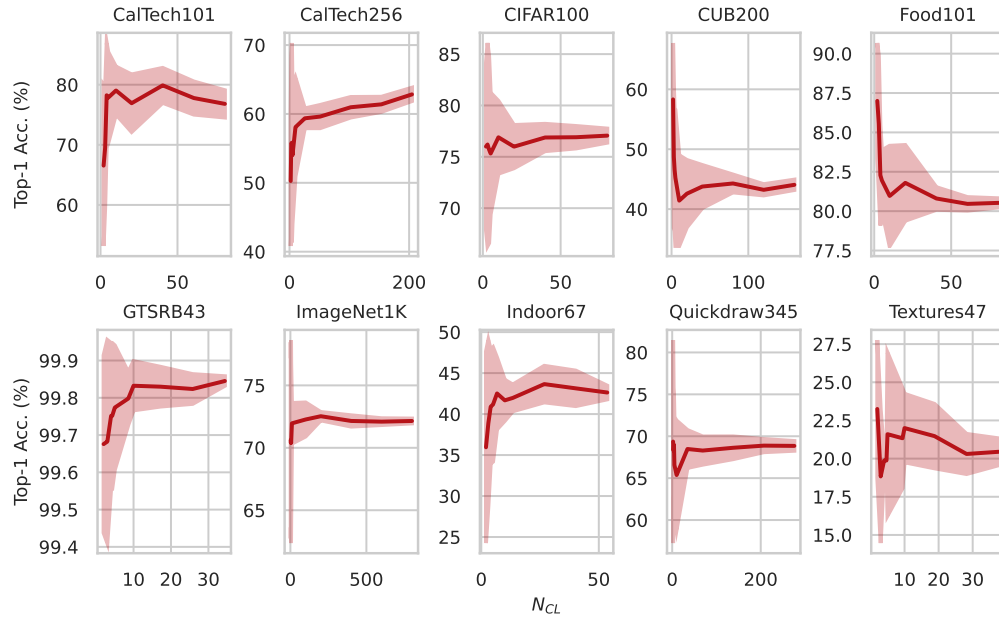
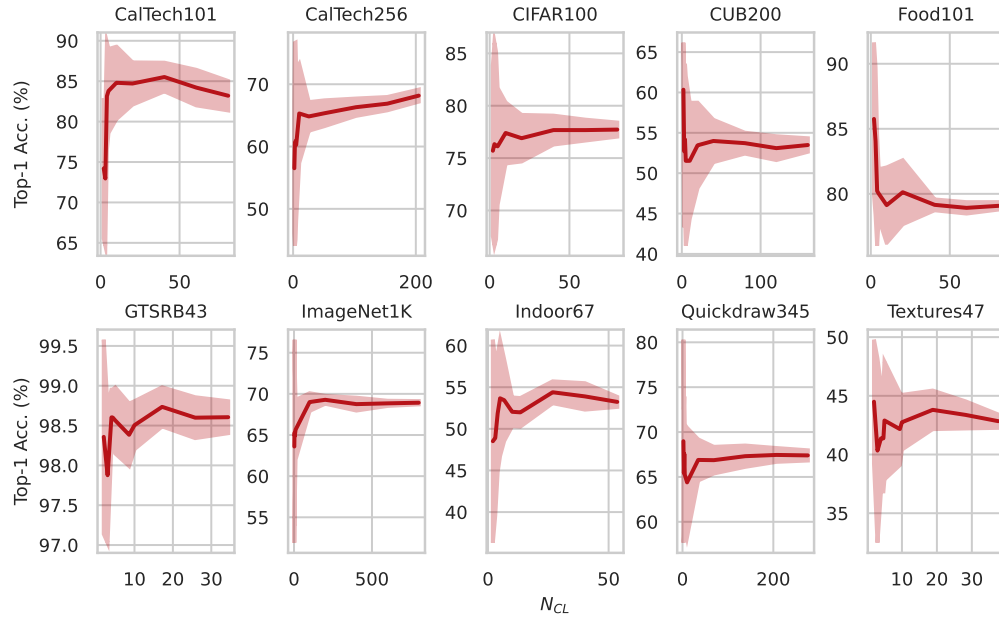Figure 12: FC-Full Top-1 Accuracy (%) for EfficientNet V2 Medium.

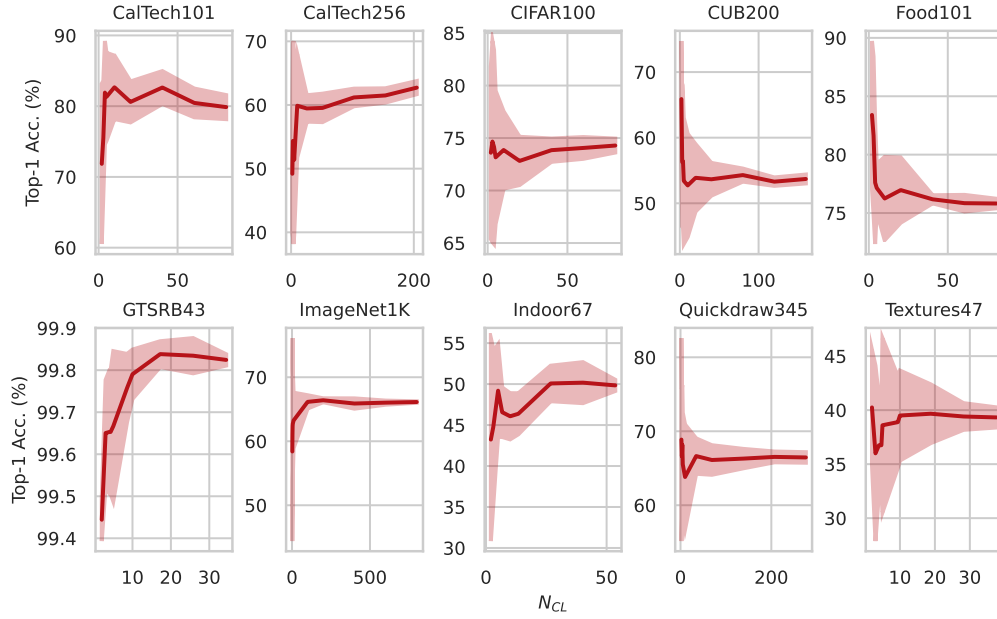Figure 13: FC-Full Top-1 Accuracy (%) for ShuffleNet V2.

23

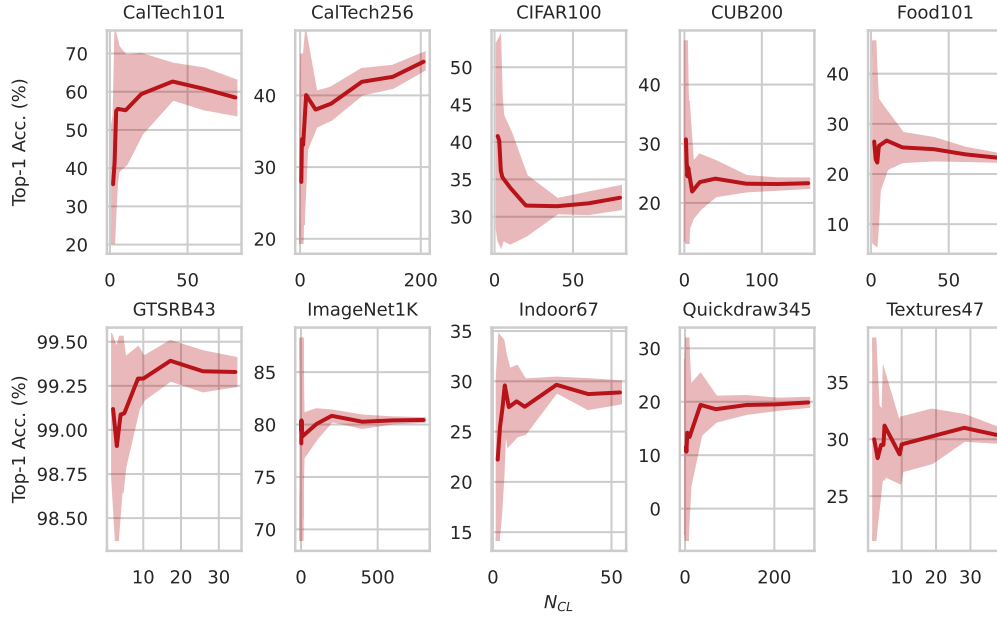Figure 14: FC-Full Top-1 Accuracy (%) for MobileNet V3 Small.

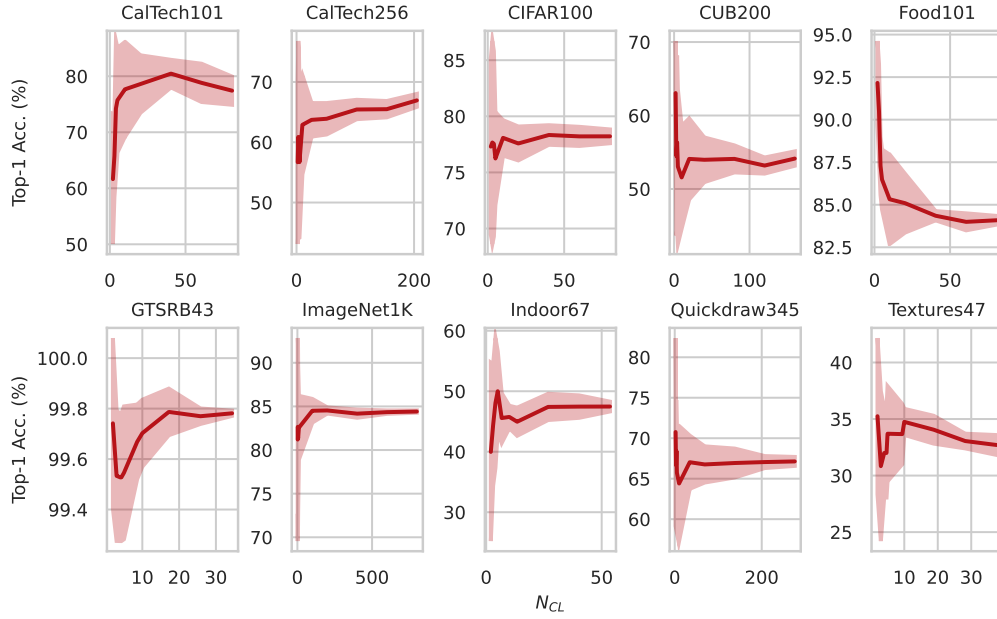Figure 15: FC-Full Top-1 Accuracy (%) for ViT Base.

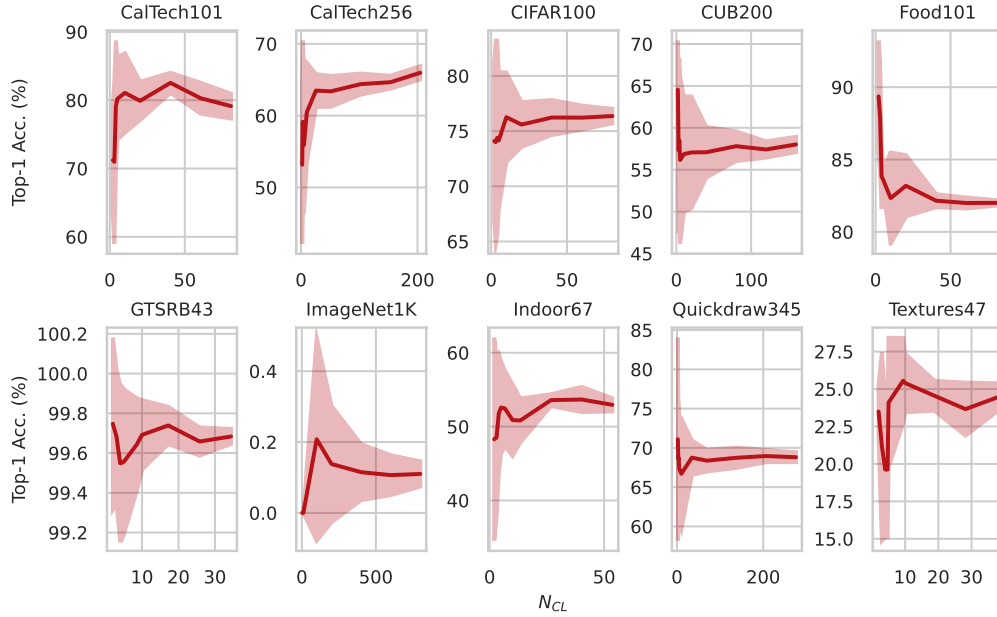Figure 16: FC-Full Top-1 Accuracy (%) for Swin V2 Base.

Figure 17: FC-Full Top-1 Accuracy (%) for MobileNetViT Small.

A.9 EXTENDED FEW-CLASS SIMILARITY BENCHMARK (FC-SIM) DETAILS

We present the extended mathematical details of 3.6 Few-Class Similarity Benchmark (FC-Sim) in the main paper.

The basic similarity formulation is adopted from (Cao et al., 2023). Notations are defined as follows:

Dataset D: a set of image instances in a dataset.

Class C: a set of image instances in a class and $|C|$ is the number of instances within class C.

Class Label L: a set of class labels in a dataset and $|L|$ is the number of classes in a dataset.

Feature Z_i: visual feature of an image and i is the instance index.

Class Pair $P^{(D)}$: a set of distinct class pairs in a dataset D; $|P^{(D)}|$ is the total number of distinct class pairs.

Intra-Class Image Pair $P^{(C)}$: a set of distinct image pairs in a class C; $|P^{(C)}|$ is the total number of distinct image pairs.

Inter-Class Image Pair $P^{(C_1,C_2)}$: a set of distinct image pairs in two classes C_1, C_2; $|P^{(C_1,C_2)}|$ is the total number of distinct image pairs. Note that this does not include same-class pairs.

Intra-Class Similarity $S_\alpha^{(C)}$: a scalar describing the similarity of images within a class by taking the average of all the distinct class pairs in C:

$$S_\alpha^{(C)} = \frac{1}{|P^{(C)}|} \sum_{i,j \in C;\ i \neq j} \cos(\mathbf{Z}_i, \mathbf{Z}_j). \tag{5}$$

Inter-Class Similarity $S_\beta^{(C_1,C_2)}$: a scalar describing the similarity among images in two different classes C_1 and C_2:

$$S_\beta^{(C_1,C_2)} = \frac{1}{|P^{(C_1,C_2)}|} \sum_{i \in C_1, j \in C_2} \cos(\mathbf{Z}_i, \mathbf{Z}_j), \tag{6}$$

where C_1 and C_2 are distinct classes, i and j are the image instance indices in C_1 and C_2, respectively. $P^{(C_1,C_2)}$ is the set of distinct pairs of images between C_1 and C_2.

The above equations formulate class-level similarity scores. For dataset-level, Intra-Class Similarity and Inter-Class Similarity of a dataset D are defined as the mean of their similarity scores, respectively:

$$S_\alpha^{(D)} = \frac{1}{|L|} \sum_{l \in L} S_\alpha^{(C_l)} = \frac{1}{|L| \times |P^{(C_l)}|} \sum_{l \in L} \sum_{i,j \in C_l;\ i \neq j} \cos(\mathbf{Z}_i, \mathbf{Z}_j), \tag{7}$$

$$S_\beta^{(D)} = \frac{1}{|P^{(D)}|} \sum_{a,b \in L; a \neq b} S_\beta^{(C_a,C_b)} = \frac{1}{|P^{(D)}| \times |P^{(C_1,C_2)}|} \sum_{a,b \in L;\ a \neq b} \sum_{i \in C_1, j \in C_2} \cos(\mathbf{Z}_i, \mathbf{Z}_j). \tag{8}$$

Averaging these similarities can provide a summary of score in class or dataset levels by a single scalar. However, this simplicity neglects other cluster-related information that can better reveal the underlying dataset difficulty property of a dataset. In particular, the **(1) tightness of a class cluster** and **(2) distance to other classes** of class clusters, are features that characterize the inherent class difficulty, but are not captured by S_α or S_β alone.

To compensate the aforementioned drawback, we adopt the Silhouette Score (SS) (also called Silhouette Coefficient in the literature) (Rousseeuw, 1987; Shahapure & Nicholas, 2020):

$$SS(i) = \frac{b(i) - a(i)}{max(a(i), b(i))}, \tag{9}$$

where $SS(i)$ is the Silhouette Score of the data point i, $a(i)$ is the average dissimilarity between i and other instances in the same class, and $b(i)$ is the average dissimilarity between i and other

data points in the closest different class. Intuitively, this metric summarizes the quality of clusters jointly by the degree of instances of the same class and distinct clusters, normalized by the longest distance of $a(i)$ and $b(i)$. By this definition, we can see that $-1 \leq SS(i) \leq 1$ where -1 indicates a dataset is poorly clustered (data points with different classes are scattered around) while 1 represents a well-clustered dataset.

Euclidean Distance is commonly used to measure two data points' differences; in contrast, we incorporate the inverse of similarity (dissimilarity) as data point's difference into the existing Silhouette Score. Observe that the above Intra-Class Similarity $S_\alpha^{(C)}$ already represents the tightness of the class (C), therefore $a(i)$ can be replaced with the inverse of Intra-Class Similarity $a(i) = -S_\alpha(i)$. For the second term $b(i)$, we adopt the previously defined Inter-Class Similarity $S_\beta^{(C_1, C_2)}$ and introduce a new similarity score as follows:

Nearest Inter-Class Similarity $S'^{(C)}_\beta$: a scalar describing the similarity among instances between class C and the closest class of each instance in C:

$$S'^{(C)}_\beta = \frac{1}{|P^{(C,\hat{C})}|} \sum_{i \in C, j \in \hat{C}} \cos(\mathbf{Z}_i, \mathbf{Z}_j), \tag{10}$$

where $\hat{C}$ is the set of the nearest class to C ($\hat{C} \neq C$).

Consequently, the dataset-level Nearest Inter-Class Similarity $S'^{(D)}_\beta$ is expressed as:

$$S'^{(D)}_\beta = \frac{1}{|L|} \sum_{l \in L} S'^{(C_l, \hat{C}_l)}_\beta = \frac{1}{|L| \times |P^{(C_l, \hat{C}_l)}|} \sum_{l \in L} \sum_{i \in C_l, j \in \hat{C}_l} \cos(\mathbf{Z}_i, \mathbf{Z}_j). \tag{11}$$

The second term of $SS(i)$ can be written as $b(i) = -S'_\beta(i)$.

Replacing $a(i)$ and $b(i)$ from equation 9 with these similarity terms, we introduce our novel similarity metric:

Similarity-Based Silhouette Score $SimSS$:

$$SimSS(i) = \frac{S_\alpha(i) - S'_\beta(i)}{max(S_\alpha(i), S'_\beta(i))}, \quad \text{for instance } i \tag{12}$$

$$SimSS^{(C)} = \frac{1}{|C|} \sum_{i \in C} SimSS(i) = \frac{1}{|C|} \sum_{i \in C} \frac{S_\alpha(i) - S'_\beta(i)}{max(S_\alpha(i), S'_\beta(i))}, \quad \text{for class } C \tag{13}$$

$$\begin{aligned}
SimSS^{(D)} &= \frac{1}{|L|} \sum_{l \in L} SimSS^{(C_l)} = \frac{1}{|L| \times |C_l|} \sum_{l \in L, i \in C_l} SimSS(i) \\
&= \frac{1}{|L| \times |C_l|} \sum_{i \in C_l} \frac{S_\alpha(i) - S'_\beta(i)}{max(S_\alpha(i), S'_\beta(i))}, \quad \text{for dataset } D.
\end{aligned} \tag{14}$$

A.10 EXTENDED FEW-CLASS SIMILARITY BENCHMARK (FC-SIM) RESULTS

We present the relationship of similarity scores using our proposed SimSS and number of classes N_{CL} in ten datasets. CLIP and DINOv2 are used as similarity base functions of SimSS shown in Fig. 18 (a) and (b), respectively.

Overall, a key observation is that the general trend among all ten datasets unveils the inverse relationship between similarity and the number of classes. Specifically, image similarities, which act as proxy of inverse subset difficulty score increases as the number of classes N_{CL} decreases. This reveals that similarity plays a more important role in the *Few-Class Regime* than for datasets with more classes. Therefore, for real applications with few classes, simply downscaling a model blindly without considering class similarity may yield a model selection with sub-optimal efficiency. We propose, therefore, that image similarity must be taken into consideration for existing scaling laws (Kaplan et al., 2020; Rae et al., 2021; Zhai et al., 2022). To that end, *Few-Class Arena*s developed to facilitate future research in this direction.
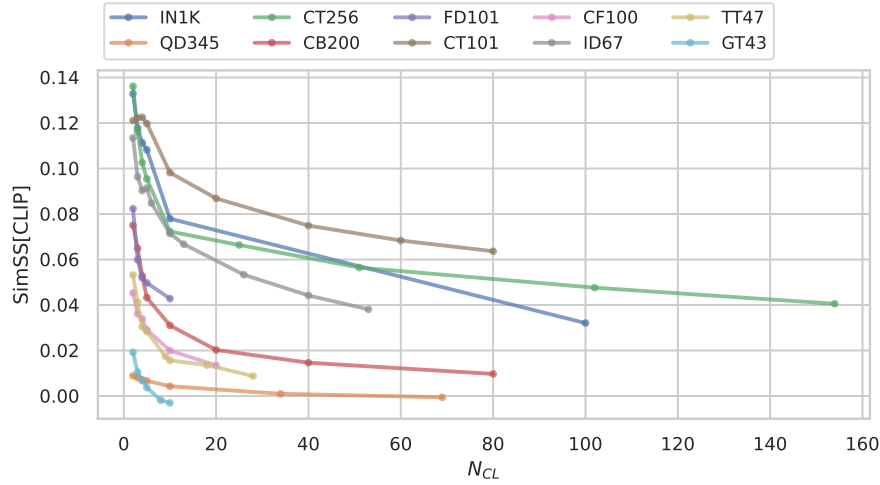
(a) SimSS using CLIP as similarity base function vs N_{CL} curve.
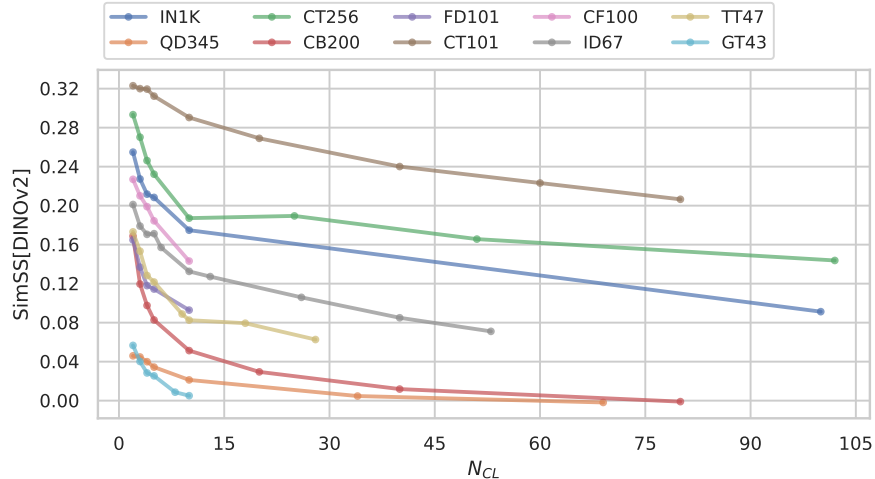
(b) SimSS using DINOv2 as similarity base function vs N_{CL} curve.

Figure 18: Relation of SimSS[CLIP,DINOv2] and N_{CL}.

Note that both CLIP and DINOv2 are trained on images from the Internet similar to ImageNet. Therefore to what extent they can capture image similarity in different types is an open research

question. Examples include drawings without textures in the Quickdraw dataset (QD345), textures without shapes in the Describable Textures Dataset (TT47), etc. We mentioned this limitation also in the main manuscript.

Effect of ResNet Scales on Similarity. We present the details of FCA-Sim results of the ResNet family in different scales in the *Few-Class Regime* of ImageNet1K, specifically ($N_{CL} \in \{2, 3, 4, 5, 10, 100\}$) shown in Fig. 19. In particular, we analyze the relationship between each full and sub-Model's Top-1 accuracy and SimSS by Pearson correlation coefficient (PCC) denoted as r in the plots. The ResNet family scales from ResNet18 to ResNet152. We experiment both CLIP (red in the first two rows) and DINOv2 (blue in the last two rows) as similarity base functions.

(a) ResNet18 (b) ResNet34 (c) ResNet50 (d) ResNet101 (e) ResNet152

(f) ResNet18 (g) ResNet34 (h) ResNet50 (i) ResNet101 (j) ResNet152

(k) ResNet18 (l) ResNet34 (m) ResNet50 (n) ResNet101 (o) ResNet152

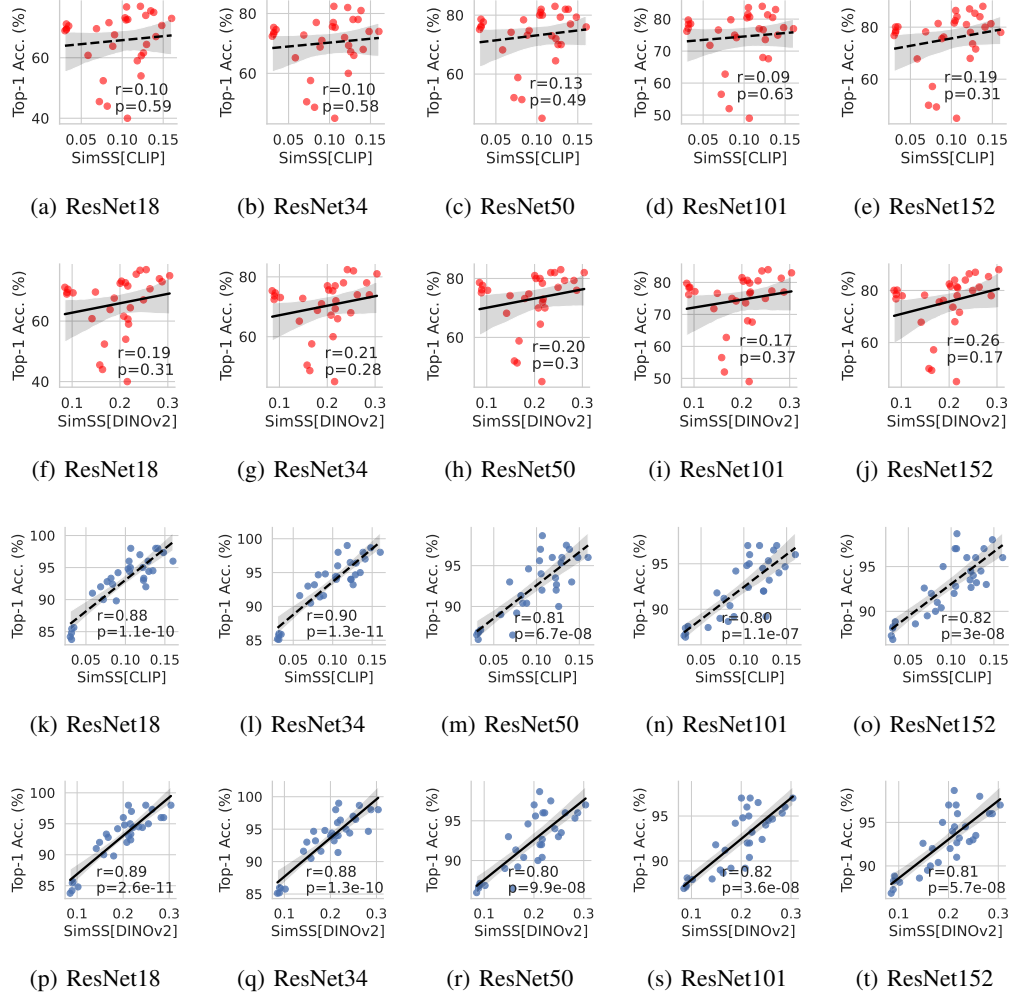(p) ResNet18 (q) ResNet34 (r) ResNet50 (s) ResNet101 (t) ResNet152

Figure 19: Top-1 Accuracy of different ResNet scales vs SimSS on ImageNet1K. $N_{CL} \in \{2, 3, 4, 5, 10, 100\}$.

In general, ResNet presents high correlation ($r \geq 0.80$) between sub-models' performances and SimSS (blue in the last two rows), compared to full models' performances and SimSS ($r \leq 0.26$, red in the first two rows). This high correlation indicates that SimSS can be used as a reliable tool to estimate upper bound accuracies of ResNet sub-models. Comparing CLIP (r in the 1st row) with DINOv2 (r in the 2nd row) as similarity base functions, observe that PCC is slightly higher for DINOv2 on full models than CLIP, while these differences are subtle for sub-models (r in the 3rd row vs 4th row). Regarding sub-models of ResNet in different scales, the two smallest models' accuracies (ResNet18 and ResNet34) have higher correlation with SimSS ($r \geq 0.88$), compared to

larger models with (ResNet50, ResNet101 and ResNet152) $r \geq 0.80$. We opens a new direction of novel scaling law considering image similarity for efficient models in *Few-Class Regime*.

Transformer vs Similarity. We present the details of Vision Transformer (ViT) (Dosovitskiy et al., 2020) Base performance and SimSS using CLIP and DINOv2 in the subsets of $N_{CL} \in \{2, 3, 4, 5, 10, 100\}$ in ImageNet1K, shown in Fig. 20. An overview of the results indicates low correlation between Top-1 accuracy and SimSS ($r \leq 0.20$). Our tool *Few-Class Arena* helps discover the new challenge of using the vanilla ViT in the *Few-Class Regime*, as ViTs are originally designed to scale up (Zhai et al., 2022) when large training datasets in the order of billion samples are available. *Few-Class Arena* also identifies the importance of scaling down considering similarity.
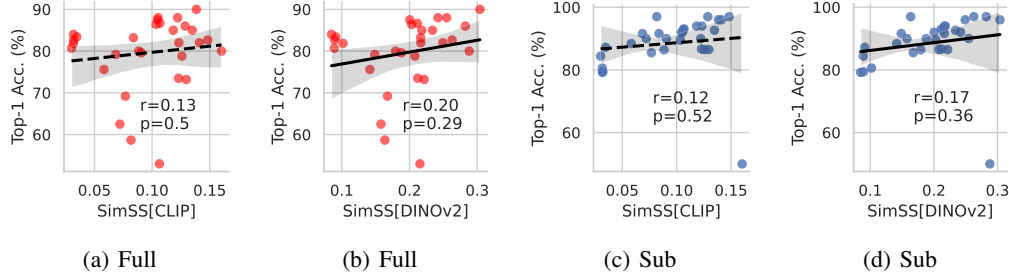

| (a) Full | (b) Full | (c) Sub | (d) Sub |

Figure 20: Top-1 Accuracy of ViT Base vs SimSS on ImageNet1K. $N_{CL} \in \{2, 3, 4, 5, 10, 100\}$.

A.11 COMPARING VARIOUS ARCHITECTURES

We perform experiments on CNNs (ResNet18, 50) and Vision Transformer-Base (ViT-B). Results are summarized in Table 7. The overall trend of ViT-B exhibists consistent with the observations in ResNet desribed in Fig. 1.

MT	N_{CL}	ResNet18		ResNet50		ViT-B	
		Top-1 Acc.↑	STDEV↓	Top-1 Acc.↑	STDEV↓	Top-1 Acc.↑	STDEV↓
F	1000	69.90	0	76.55	0	82.37	0
F	10	66.68	4.372	73.76	3.675	79.52	2.704
F	5	65.68	9.680	72.16	9.302	79.12	8.146
F	2	62.80	14.18	70.60	14.67	78.00	14.47
S	10	91.88	1.640	91.48	2.265	82.16	3.508
S	5	93.68	1.213	92.96	3.170	89.60	2.227
S	2	96.80	1.304	94.80	2.168	95.60	1.949

Table 7: Performance results for different models and configurations on ImageNet1K. $N_{CL} \in \{2, 5, 10, 1000\}$, MT: Model Type, F: Full model, S: Sub-model.

A.12 EXTENSION TO OBJECT DETECTION AND SEGMENTATION

To assess the generalization of the few-class properties to Object Detection (OD) and Segmentation (Seg), we conducted additional validation experiments using YOLOv8. The procedure is consistent with the method outlined in Section 3.3 and 3.4. Specifically, for a specific N_{CL} (2 in this example), we randomly sample the N_{CL} classes from the full dataset of COCO, where each consists of five subsets with seed numbers from 0 to 4. We performed experiments with 2, 5, 80. The YOLOv8-nano model was chosen since we focus on efficiency. Image size of 320x320 was used. Model performance was evaluated using the standard metric, mean average precision at an IoU threshold of 0.5 (mAP@50). Table 8 summarizes our results:

We also include a comparison with fine-tuned pre-trained models (denoted as F). These models are initialized with weights from the pre-trained YOLOv8-nano on the full dataset with 80 classes, and subsequently fine-tuned for a limited number of epochs (five in this example). We conclude that OD and Seg task exhibit similar observations we make in Fig. 1.

MT	N_{CL}	OD		Seg	
		mAP@50↑	STDEV↓	mAP@50↑	STDEV↓
F	80	0.405	0.195	0.378	0.200
F	5	0.456	0.090	0.435	0.098
FT	5	0.488	**0.069**	0.465	0.082
S	5	**0.503**	0.069	**0.474**	**0.084**
F	2	0.488	0.161	0.475	0.180
FT	2	0.505	0.127	0.457	0.159
S	2	**0.538**	**0.106**	**0.482**	**0.152**

Table 8: Performance results for different tasks and configurations on COCO. $N_{CL} \in \{2, 5, 80\}$, MT: Model Type, OD: Object Detection, Seg: Segmentation, F: Full model, S: Sub-model, FT: Fine-tuned model. Best scores are highlighted in bold. The gray bar indicates sub-models as the primary focus of this research.

A.13 EXPERIMENTS COMPUTE RESOURCES

Experiments are conducted in two internal clusters with the following specifications: (1) 8 NVIDIA RTX A5000 24GB, AMD EPYC 7513 32-Core Processor 882GB RAM and (2) 8 NVIDIA TITAN Xp 12GB, Intel(R) Xeon(R) CPU E5-2650 v4 @ 2.20GHz, 126GB RAM. When GPUs in two clusters are fully utilized, training 10 models in 9 datasets takes 2 weeks; obtaining one experiment result of FC-Full usually takes less than 1 minute since it only involves inference without training; obtaining one experiment result of FC-Sub takes around 2 days on average depending on the size of subset and model, which includes both training and testing; computing the SimSS in the *Few-Class Regime* for ten datasets takes around three weeks.

A.14 LIMITATIONS AND FUTURE WORK

The current difficulty benchmark supports image similarity while in the future it can be expanded to other difficulty measurements (Scheidegger et al., 2021). CLIP and DINOv2 are trained toward general visual features, it is unclear if they will be appropriate for other types of images such as sketches without textures in Quickdraw (Ha & Eck, 2017) . For this reason, a universal similarity foundation model would be appealing that applies to any image type. In summary, *Few-Class Arena* identifies a promising new path for achieving efficiencies focused on the important and practical *Few-Class Regime*, establishing a baseline for future work.